N84 25756

Application of Surface Acoustic Wave Devices to Radio Telemetry

Final Report covering period:
Jan. 1, 1981 to Dec. 15, 1983

Principal Investigator: Udo Strasilla
NASA Technical Officer: Gordon J. Deboo
Grant No. NAG 2-85

Application of Surface Acoustic Wave Devices to Radio Telemetry

Final Report
covering the period:
Jan. 1, 1981 to Dec. 15, 1983

Principal Investigator: Udo Strasilla
Assoc. Professor
Dept. of Elec. Engr.
San Jose State Univ.
San Jose, CA 95192

NASA Grant No. NAG 2-85

NASA Technical Officer: Gordon J. Deboo
Chief, Electronic Instrument
Development Branch
Mail Stop 213-3
Ames Research Center
Moffett Field, CA 94035

NASA Grant Support

The bulk of the project reported here was supported by Grant No. NAG 2-85, grant period 1/1/81 to 9/30/82.

The manufacture of the SAWR devices generated at SJSU was funded by Grant No. NCC 2-143, with Prof. Chen Yuen as principal investigator and with a grant period 5/11/81 to 11/30/82.

In order to achieve the stated goal additional work had to be performed during the Fall semester 1983. A portion of this investigation was supported by grant No. NAG 2-215 (grant period: Dec. 82 to Dec. 84.)

A follow-up grant, based on the work supported by above grants was awarded to Prof. Yuen. The object of this grant, No. NAG 2-280, with a grant period from 2/10/84 to 2/28/85, is to manufacture a hybrid SAW oscillator, containing a 180 MHz SAWR and the associated circuitry.

Summary

The original intent of this grant was

1. to obtain commercial Surface Acoustic Wave Resonator (SAWR) devices,
2. to reconstruct and experiment with coventional oscillators in order to gain more experience with different oscillator configurations,
3. to construct and evaluate an oscillator using a SAW resonator.

Since no commercial SAWR devices were available to the start of the grant period, additional steps had to be taken to achieve the goal. A parallel grant (Grant No. NCC 2-143) was obtained by my colleague, Prof. Chen Yuen, for the manufacture of SAWR's in our Integrated Circuits facilities. Prior to the manufacture of these devices different low frequency oscillators were investigated, for example the lumped element (LC) delay line oscillator, the single transistor Colpitts oscillator and the tuned gate junction FET oscillator. Also, in order to obtain experience in the high frequency region a two stage oscillator-filter (in the Clapp configuration) tuning in on the 3rd harmonic of a 20 MHz crystal, was experimented with. In an effort to better understand the input-output characteristic of a SAW device, the filtering behavior of a Crystal Technology CTI 55B SAW filter was tested.

Initial measurements on the first run SAWR device manufactured at SJSU using the impulse response method showed very high attenuation. Sustained oscillation could not be obtained when using the device in a delay line oscillator configuration with a two stage amplifier. In a second production run of SAWR's the ion was decreased by closer spacing of the input/output interdigital transducers (IDT), and the desired center frequency near 180 MHz could be achieved. This device, however, has only a small peak on top of a too broad bandwidth, making its application for an oscillator impracticable. The spurious peaks and broadening

of the bandwidth appears to be caused by random reflections of the surface wave from the edges of the device, overshadowing the forced reflections by the seven reflections on each side. The importance of the reflection was demonstrated by the 3rd run device, where the reflections have been left out completely while the IDT structure was more finely tuned. Latter devices showed no peaking at all.

Finally, a commercial 280 MHz SAWR could be obtained from Hewlett Packard. Special arrangements were made to receive a few "reject" devices, devices which did not meet HP's tight frequency specifications, since these devices are not sold outside; they are made only for one of HP's own instruments. Using this high Q resonator in a common-base Colpitt's configuration, its capability to stabilize the oscillation frequency of a resonating circuit was demonstrated.

Thus, it was shown that a SAWR stabilized oscillator is superior to the crystal controlled oscillator particularly in radio telemetry applications in biological space shuttle experiments where low power, light weight and small size is important. It was demonstrated that a SAWR with the desired 180 MHz frequency can be manufactured by using the same IDT spacing as before, by placing the input and output IDT's in close vicinity for strong coupling and by using a large number of reflections for the achievement of standing waves. Based on the achievements of this grant (NAG 2-85) and Professor Yuen's parallel grant NCC 2-143 the foundation was laid for Professor Yuen's grant NAG 2-280 for the manufacture of a hybrid SAWR oscillator containing SAWR and circuitry on one device.

Contents of Report

The work done is described in more detail in the reports attached.

Part 1: "Simulating a SAW Oscillator Using a Lumped Element LC Delay Line", by Timothy Upshaw, Dec. 6, 1981.

Part 2: "SAW Oscillator Design Project" by Michael Williamson, May 16, 1982.

Part 3: "Evaluation of a Surface Acoustic Wave Resonator Manufactured at San Jose State University", by Andreas Gulle, Dec. 15, 1983.

Appendix: Interim Status Report covering period Feb. 1, 1981 to Sept. 30, 1981.

Abstracts of the Reports

Part 1: "Simulating a SAW Oscillator Using a Lumped Element LC Delay Line", by Timothy Upshaw, Dec. 6, 1981.

The lumped element (LC) delay line is analogous to the SAW (Surface-Acoustic-Wave) device because they both have the ability to delay the signal. This paper analyzes an oscillator constructed from a lumped element delay line to compare it with the SAW oscillator. The LC oscillator is frequency variable (depending on the delay tap) and contains only two elements: the LC delay line and a NAND gate. This paper describes delay line theory, analyzes the delay line oscillator, and discusses the SAW device as an oscillator.

Part 2: "SAW Oscillator Design Project", by Michael Williamson, May 16, 1982.

A review of oscillator theory is given, and, in particular, the single transistor Colpitts oscillator and the tuned-gate junction FET oscillator are discussed. It is shown that, though crystals may be used for the stabilization of the oscillators up to about 200 MHz, harmonics have to be used at frequencies higher than 20 MHz. Thus the use of Surface Acoustic Wave Resonators (SAWR's) promise more simple circuitry in higher frequency regions. After giving a brief qualitative explanation of the principle of SAW's, the two most common types of SAW oscillators, the SAW delay line and the SAW resonator oscillator are discussed.

A two stage 60 MHz oscillator-filter-amplifier circuit using the 3rd harmonic of a 20 MHz crystal was constructed and evaluated, in order to gain more experience with high frequency oscillators. In an effort to better understand the input-output characteristics of a SAW device, the filtering behavior of a commercial bandpass SAW filter was tested.

Tests conducted on a SAW manufactured at the SJSU integrated circuits facilities showed about 70 dB attenuation. In an attempt to use this device in a two stage SAW oscillator configuration sustained oscillations could not be achieved.

Part 3: "Evaluation of a Surface Acoustic Wave Resonator Manufactured at San Jose State University", by Andreas Gulle, Dec. 15, 1983.

Three experimental Surface Acoustic Wave Resonators (SAWR's), manufactured at the SJSU Integrated Circuits Lab facilities were evaluated. The devices were intended to be used for the frequency stabilization of a 180 MHz oscillator. For a reference, measurements were made on a commercial 280 MHz SAWR from Hewlett Packard, as well as on a Crystal Technology SAW bandpass filter. Frequency and phase response as well as the input/output impedance of the devices were correlated with their geometries and equivalent circuits.

The first batch of SAWR devices manufactured at SJSU, using two electrode pairs and seven reflectors, showed a high loss due to the large distance between the interdigital transducers (IDT's). From the second run, where the number of electrode pairs was increased to 15, and where the distance between the IDT's was reduced by a factor of two, useful measurements could be obtained. The transfer function displayed a center frequency close to the desired 80 MHz frequency, indicating correct spacing of the electrode pairs. The bandwidth of 8 MHz, however, was too wide causing the device to be useless as a resonator. The multiple secondary resonance peaks probably are caused by multiple superimposed reflections of the surface wave from the edges of the device. The importance of reflectors is demonstrated in a third run, where the spacing of the IDT's was improved, but where the reflectors were omitted, resulting in the disappearance of a distinct resonance peak.

This study showed that a desired center frequency was obtained due to correct spacing of the IDT's, that the transmitting and receiving IDT's

have to be close for sufficient coupling and that a large number (about 100) reflectors are required for the creation of a standing wave resulting in a high Q-value.

That a SAW device can be used for stabilizing the oscillation frequency of a resonating circuit was demonstrated by using a commercial high Q 280 MHz resonator from Hewlett Packard in a common-base Colpitts configuration. The advantage of using a SAW device for oscillator stabilization is obvious when considering that the 11th harmonic of a bulk acoustic wave crystal would have to be used in order to achieve the same oscillation frequency.

Appendix: Interim Status Report covering period Feb. 1, 1981 to Sept. 30, 1981.

In this report the difficulty in obtaining commercial SAW resonators is described. Only SAW filters could be obtained which were used for exploratory measurements. The initial phase of the work of two students experimenting with different oscillator configurations and doing a preliminary assessment of an experimental SAWR manufactured at SJSU is illuminated.

SAW Oscillator Design Project

by
Michael Williamson

San Jose State University
May 16, 1982

TABLE OF CONTENTS

Introduction

Wide application for SAW oscillators has been predicted because of their simple fabrication capability and direct oscillation in the UHF band. This paper deals first with the operation of conventional LC and quartz crystal oscillator circuits and, second, with the construction of an oscillator which utilizes a SAW resonator as the frequency determining element within the oscillator circuit. The frequency of the SAW resonator is determined by the spacing of its grooved reflectors. Since the resonator may be fabricated on a single substrate, the oscillator can be mass-produced using photolighography.

Oscillators

The overall behavior of sinusoidal oscillator circuits is determined by the frequency and amplitude-determining mechanisms of the given circuit. These mechanisms are characterized by their stability as a function of time, temperature, supply voltage and the interrelationships between amplitude and frequency.

At a minimum, all sine-wave oscillators must contain

1) an active device with power gain at the operating frequency,

2) a frequency-determining element or network, and

3) an amplitude-limiting and stabilizing mechanism.

While sinusoidal signals can be produced by filtering separately produced square waves, or impulse chains or by shaping techniques applied to triangular wave, only sinusoidal oscillations produced by linear feedback will be treated here.

Of paramount importance to sustaining of sinusoidal oscillations in conventional oscillators is the existence of a pair of complex conjugate poles in the right half complex plane when power is first applied at $t = 0$. When excited by thermal noise or the step generated by switching on the power, these unstable poles will give rise to a sinusoidal output voltage with an exponentially increasing amplitude envelope. Since the objective is to produce a sustained constant amplitude sinusoidal output, this envelope cannot grow indefinitely. Thus, as the envelope of the sinewave increases, it must cause a change in the value of one or more of the network parameters in such a way that the complex conjugate poles are driven toward the imaginary axis. This is usually accomplished by altering the amplification of the oscillator circuit. In effect, the amplitude of the sinusoid increases until the complex conjugate poles

lie on the imaginary axis and a constant amplitude sinusoidal output results. If for any reason the amplitude continues to increase, the poles move into the left half plane causing a decrease in amplitude until the poles again lie on the imaginary axis. Likewise, a decrease in the required sinusoidal amplitude will cause the poles to move back into the right half plane. Again the amplitude will increase until the poles are positioned on the imaginary axis.

The basic requirements for a sinusoidal oscillator are now clear. We need a network with a pair of small-signal complex conjugate poles which determine the frequency of oscillation, and a mechanism for moving the poles toward the imaginary axis whenever the envelope of the sinusoid deviates from the desired amplitude. In order to obtain right-half plane poles, we require positive feedback such that the output and input are in phase at the frequency of oscillation. The figure below illustrates a generalized feedback amplifier.

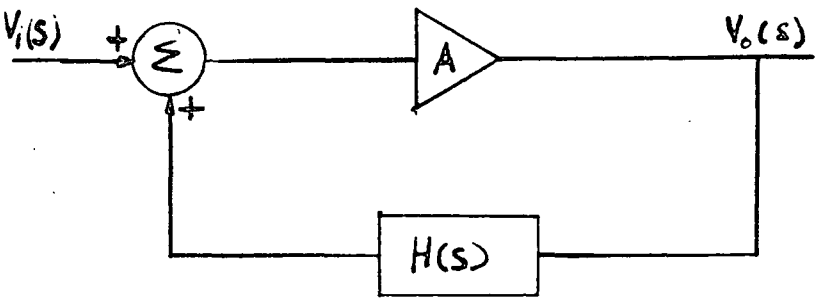

Figure 1. Positive Feedback Amplifier

The transfer function is given by $\frac{V_o(s)}{V_i(s)} = \frac{A}{1 - AH(s)}$

where AH(s) is defined as the loop gain. In order for the oscillator circuit to have a pair of complex conjugate poles in the right half plane, the zeros of $1 - AH(s)$ must include the desired pole pair.

Thus, in designing a sinusoidal oscillator we select a suitable pole zero pattern for AH(s) which causes one pair of complex conjugate roots of $1 - AH(s)$ to cross the imaginary axis at a predetermined frequency w_o as $|A|$ increases. Care must be taken not to introduce any other conjugate pairs since this will introduce unwanted oscillations. After determining the minimum magnitude of A which places the roots on the imaginary axis, A is chosen somewhat larger than this value to insure self-starting. Then, to prevent the output from increasing without bound, a non-linear device which reduces the magnitude of A as the output oscillations grow toward the desired amplitude is incorporated.

From root locus stability analysis we know that at least two open poles of $1 - AH(s)$ are required to have right-half plane complex conjugate roots. However, two poles are not a sufficient condition for oscillations to occur. If AH(s) has two poles, one zero must also exist. The simplest pole-zero configuration for AH(s) which is capable of producing right-half plane roots is shown below.

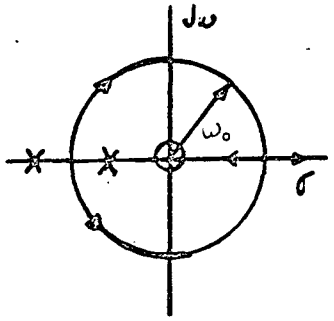

$$AH(s) = \frac{Aw_1 s}{(s+w_1)(s+w_2)}$$

Figure 2. Root Locus of AH(s) with two poles and one zero

For $A>0$ oscillations will occur when the root locus crosses the jw axis.

To find the frequency of oscillation and minimum gain we set $s = jw$ and $A = A_{min}$. When the Barkhausen criterion

$$R_e\left[AH(jw)\right] = 1,$$
$$I_m\left[AH(jw)\right] = 0$$

is invoked, we find that with

$$I_m\left[AH(jw)\right] = \frac{A_{min}\, w_1 w_0\, (w_1 w_2 - w_o^2)}{w_o^2 (w_1 + w_2)^2 + (w_1 w_2 - w_o^2)} = 0$$

The value of $w_o = \sqrt{w_1 w_2}$, where w_o is the frequency of oscillation. Then with $w_o = \sqrt{w_1 w_2}$ yields

$$R_e\left[AH(jw)\right] = \frac{A_{min}\, w_1}{w_1 + w_2} = 1,$$

from which we obtain $$A_{min} = \frac{w_1 + w_2}{w_1}$$

The small-signal circuit diagram with this pole-zero pattern is illustrated below.

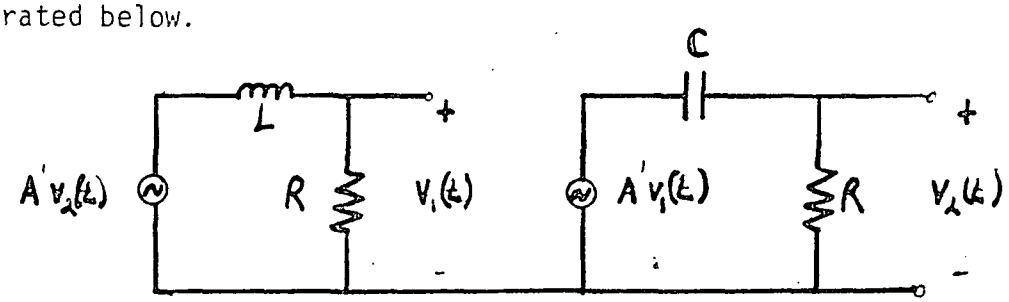

Figure 3. Small Signal Oscillator Circuit

Since $$V_1(t) = \frac{A'(R/L)}{s + R/L} V_2(t) \qquad V_2(t) = \frac{A's}{s + 1/RC} V_1(t)$$

AH(s) is given by $$AH(s) = \frac{(A')^2 (R/L)s}{(s + R/L)(s + 1/RC)};$$

Thus, $A_{min} = 1 + 2/R^2C$, $w_1 = R/L$, and $w_2 = 1/RC$. If $1/RC = R/L$ the special case results where $w_1 = w_2 = w_0 = 1/\sqrt{LC}$ and $A_{min} = 2$.

Alternatively, a pole-zero pattern with two complex conjugate left-half plane poles and a zero near or at the origin will also produce oscillations. The root locus for this case is shown below

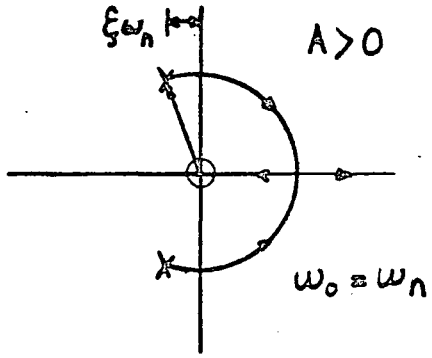

$$AH(s) = \frac{Asw_n}{s^2 + 2\xi w_n + w_n^2}$$

Figure 4. Root Locus of AH(s) with two complex conjugate poles and a zero near the origin.

Again when the Barkhausen criterion is applied, we find that with

$$I_m\left[AH(jw_o)\right] = \frac{jAw_o w_n(w_n^2 - w_o^2)}{(w_n^2 - w_o^2)^2 + 4\xi^2 w_n^2 w_o^2} = 0$$

and

$$R_e\left[AH(jw_o)\right] = \frac{Aw_o w_n(2\ w_n w_o)}{(w_n^2 - w_o^2)^2 + 4\xi^2 w_n^2 w_o^2} = 1$$

the conditions for oscillation became $w_o = w_n$ and $A_{min} = 2\xi$. Note that $2\xi = 1/Q_T$ where Q_T is the Q of the passive elements within the feedback loop. Clearly, then, as Q_T increases, the required amplification of the active element within the feedback loop decreases.

A second advantage of this pole-zero pattern over the previous example lies in the fact that frequency stability is increased by positioning the complex conjugate poles of AH(s) near the jw axis. Then if any poles and zeros should appear due to parasitic capacitance and

inductance the modified root loci will still be constrained to cross the imaginary axis relatively close to $w_o = w_n$. Viewed from the perspective of the phase shift due to the passive components, we observe, that if Q_T is high, the phase shift varies rapidly with frequency in the vicinity of w_n. This is easily shown by noting that for

$$AH(s) = \frac{Asw_n}{s^2 + 2\xi w_n s + w_n^2}$$

the phase ϕ of $AH(jw)$ in the vicinity of w_n is given by

$$\phi = -\tan^{-1} \frac{2Q_T(w-w_n)}{w_n}$$

and $\left.\frac{d\phi}{dw}\right|_{w_n} = \frac{-2Q_T}{w_n}$ when ϕ is small.

Therefore, spurious phase shifts introduced by parasitic elements in the feedback loop will require only a small change in frequency away from w_n to produce a compensating phase shift. For example, a typical quartz crystal has a Q on the order of 10,000. Thus if w_n = 20MHz, a 1^o shift in overall loop phase requires only a 17.5Hz shift in frequency to compensate.

The figure below illustrates one of many small signal oscillator circuits whose loop transfer function AH(s) contains a pair of complex poles and a zero at the origin.

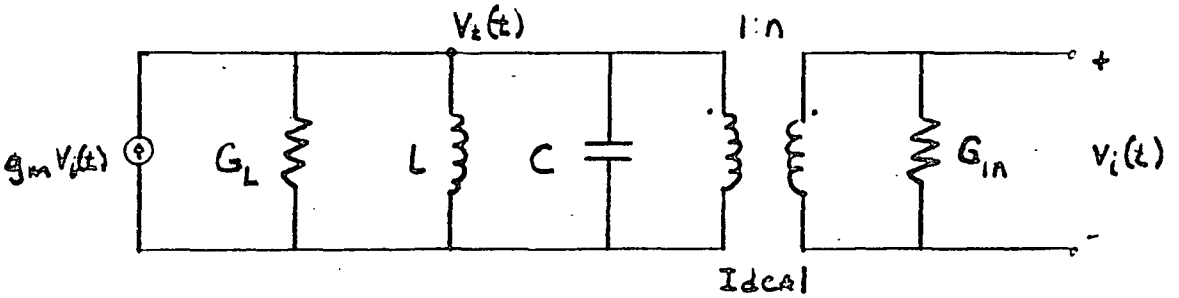

Figure 5. Oscillator Circuit with a pair of complex conjugate poles and a zero at the origin.

For this circuit

$$V_t(t) = g_m V(t) \frac{s(1/C)}{s^2 + s(G_t/C) + 1/LC}$$

$$V_i(t) = nV_t(t)$$

Thus

$$AH(s) = \frac{(\frac{ng_m}{GT})(2\xi w_n s)}{s^2+2\xi ws + w_n^2}$$

where $w_n = \sqrt{1/LC}$, $2\xi w_n = {}^{G}T/C$ and $G_T = G_L = n^2 G_{in}$

This circuit can be realized by cascading the passive elements with a common base transistor or common gate FET. In either case the minimum gm required for oscillation at $w = w_n$ is $gm = G_{T/n}$. This value decreases with decreasing G_T or, equivalently, with increasing $Q_T = w_n C/G_T$

In practice the majority of oscillators in common application are self-limiting single transistor oscillators of the form shown below.

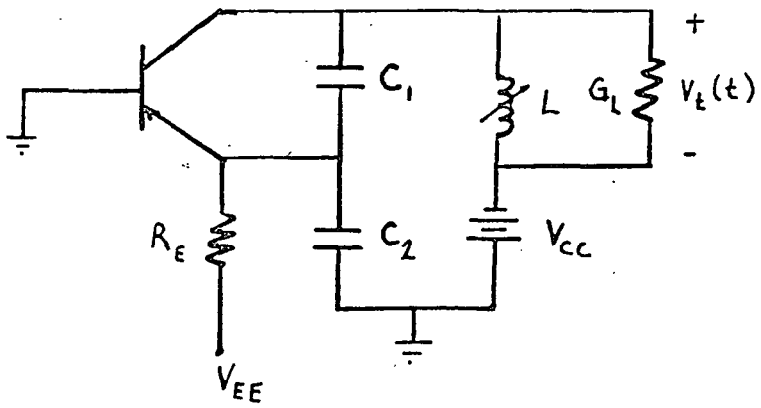

Figure 6. Single Transistor Colpitts Oscillator

In this circuit, known as a Colpitts oscillator, the tapped capacitive transformer constitutes the frequency-determining network. Other oscillator circuits which employ this same transformer-like network include the Hartley and Tuned-collector oscillator.

For the Colpitts oscillator shown above the quiescent emitter current is given by $$I_{EQ} = \frac{V_{EE} - V_{BEQ}}{R_E},$$

Thus, the small signal input conductance at the emitter is given by $g_{in_Q} = qI_{eq}/kT$ and the small signal transconductance has the form of $gm = \alpha g_{in_Q}$. If we now assume that $Q_T > 10$, $Q_E > 10$ and $nQ_TQ_E > 100$, then the capacitive transformer may be replaced by the transformer model used to illustrate AH(s) with two complex conjugate poles. That is, the Colpitts oscillator can be modeled as

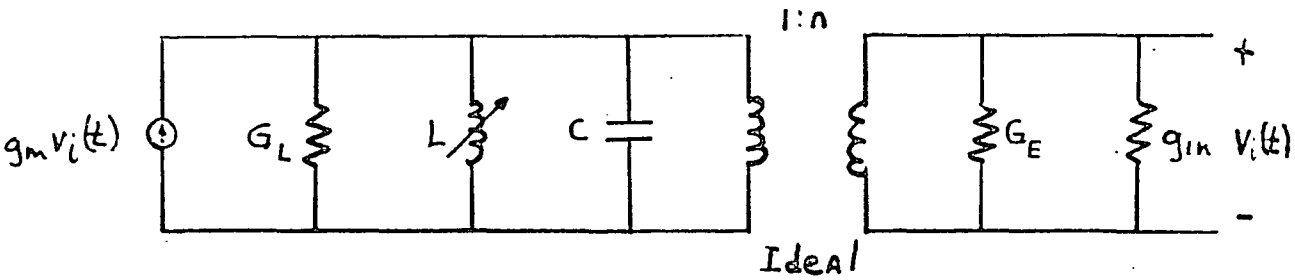

Figure 7. Colpitts Oscillator Small-Signal Model.

where $C = C_1C_2/C_1+C_2$, $n = C_1/C_1+C_2$, $gm = \alpha g_{in}$, $g_{in} = qI_{eq}/kT$,

$w_o = 1/\sqrt{LC}$, $nQ_TQ_E > 100$ and $Q_E > 10$.

Provided that $$gm_Q > gm_{Q_{min}} = \frac{G_L + n^2 G_E}{n(1-n/\alpha)}$$

The frequency of oscillation will be given by $w_o = \sqrt{1/LC}$. If the inequality holds, the oscillation grows until the transistor non-linearities manifested in K reduce AH(jw) to unity at which level the oscillation stablizes.

The use of an FET as the active element in a turned-gate oscillator possesses certain advantages, that other oscillator circuits lack. In the configuration shown below the tuned circuit has virtually no loading due to the FET.

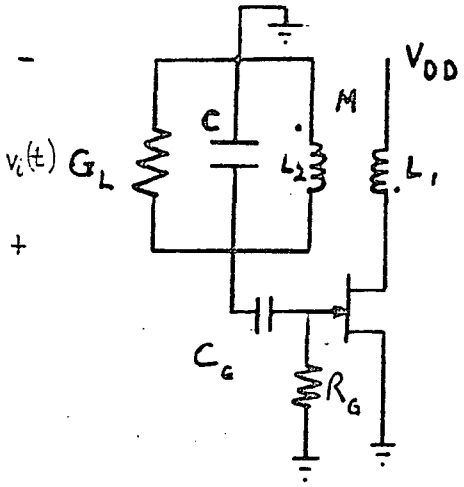

Figure 8. Tuned-gate Junction FET Oscillator

Thus, it is possible to maintain a high value of Q_T and consequently good frequency stability. Two conditions will assure this property to exist. With R_G in the nominal range of 1MΩ to 10MΩ no appreciable load is presented to the tank while if $M/L_2 \ll 1$ only a negligible amount of loading due to output impedance (both capacitive and resistive) of the FET will be reflected through the transformer. In addition the ac component of V_{DS} is kept low when $M/L_2 \ll 1$, resulting in a negligibly small "Miller effect." Therefore, the capacitive loading of the FET input directly across the tuned circuit is minimized. The Colpitts, Hartley, and tuned-drain configurations possess none of these advantages.

One interesting feature of the tuned-gate oscillator is the clamped biasing resulting from the capacitor C_G and the gate-to-source junction diode. This negative clamping circuit clamps v_{GS} to the turn-on bias of the diode, V_o. Since V_o is a function of the average diode current and an R_G of several megohms requires the average diode current to be quite small ($\sim$.1uA), V_o is usually required to be less than 0.5 volts, even for silicon. Thus, as a good first approximation we can assume $V_o \approx 0$. Thus, since C_G is an ac short at the oscillation frequency, we find that if $v_i = V_1 \cos w_o t$, then $v_{GS} = V_1 \left[(\cos w_o t) - 1\right]$. This form of bias, in contrast to the biasing obtained by inserting a negative voltage source in series with R_G, has the advantage of stablizing the oscillation amplitude with the FET operating within its square-law region. This can be quite desirable when the tuned-gate oscillator is employed in the construction of mixers since undesirable undermodulation products are minimized when the FET is operating in the square law region. With a clamped bias, the FET transconductance decreases with increasing sinusoidal input voltage amplitude within the square-law region, while for a fixed negative bias the FET transconductance remains independent of input voltage amplitude for operation completely within the square-law region.

To obtain a model of the tuned-gate circuit we observe that with $M/L_2 \ll 1$, the reflected impedance in drain circuit remains quite small. Hence, we may neglect the output resistance of the FET, V_o, when calculating the drain current. Thus, $i_D = I_{DSS}(1 - \frac{v_{GS}}{V_p})^2$

In addition, $M/L_2 \ll 1$ ensures operation within the saturation region since in this case the ac drain voltage will be quite small.

From the assumption outlined above and that Q_T of the tuned circuit is sufficiently high to keep $v_i(t)$ sinusoidal, the large-signal model for the tuned-gate FET oscillator can be found. In this model, shown below, only the fundamental component of the drain current is reflected through the transformer, because of the high Q_T. In this manner we obtain the driving current source given by $(M/L_2)(G_m V_1 \cos w_o t)$ where G_m is the large-signal fundamental transconductance of the clamp-biased FET.

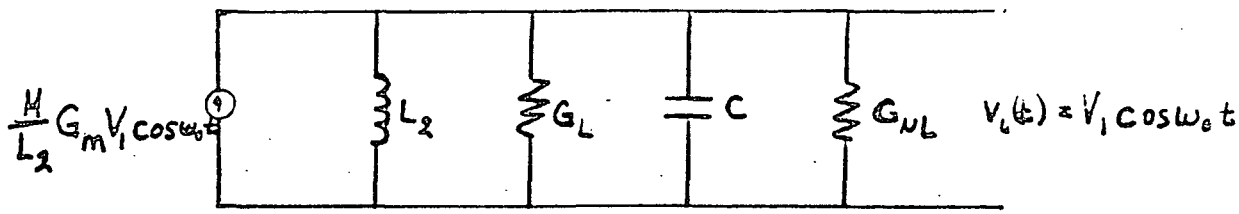

Figure 9. Tuned-gate FET Oscillator Large Signal Model

$$w_o = 1/\sqrt{L_2 C} \quad G_{NL} = 3/R_G \quad Q_T = \frac{w_o C}{G_{NL} + G_L}$$

From the large signal model we can see that

$$I_m[A_L(jw_o)] = 0 \quad \text{for} \quad w_o = 1/\sqrt{L_2 C}$$

and that

$$R_e[A_L(jw_o)] = (M/L_2)\left(\frac{G_m}{G_L + G_{NL}}\right) = 1$$

When the need for high frequency stability exists the use of a piezoelectric resonator is indicated. Used in place of a conventional L-C combination the available Q may be as much as 1000 times greater than

that of the L-C combination. Since frequency stability is directly proportional to the value at Q, quartz crystal oscillators are used whenever high frequency stability is necessary. The basic electrical model of a quartz crystal is shown below.

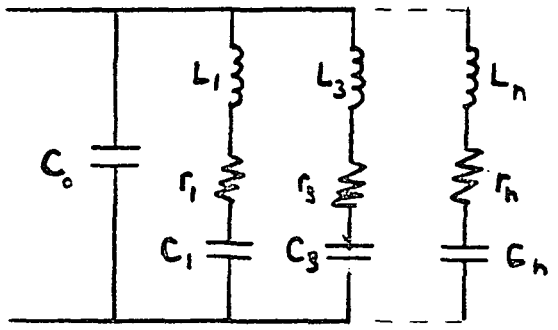

where C_o = case electrode capacitance

Figure 10. Electrical Model for a Quartz Crystal Resonator

Normally the crystal operates within 1% of the series resonant frequency of one of the shunt branches, hence the circuit is usually reduced to C_o parallel with a series shunt resonant circuit. The multiple branches result from mechanical vibrations at approximately the odd harmonics of the fundamental frequency. The existence of these overtones allows for the construction of crystal oscillators up to the neighborhood of 200MHz. Since the mechanical frequency of the fundamental vibration is proportional to the crystal dimensions, absence of these overtones would limit the fundamental frequency of vibration to approximately 20MHz. When frequencies beyond the limits of the quartz resonator are required harmonic multiplication must be employed.

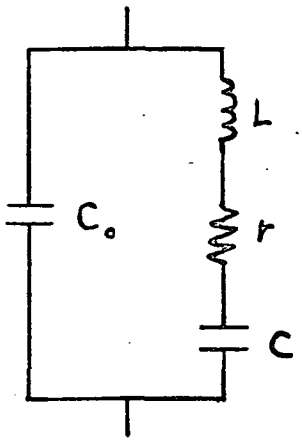

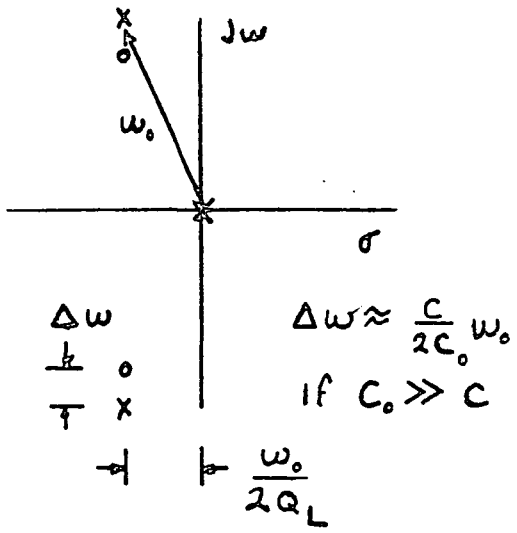

$$Z(s) = \frac{1}{sC_o}\left[\frac{s^2 + s\frac{r}{L} + w_o^2}{s^2 + s\frac{r}{L} + (1+\frac{C}{C_o})w_o^2}\right]$$

where $w_o^2 = \frac{1}{LC}$ $Q_L = \frac{w_o L}{r}$

Figure 11. Crystal Model

The figure above illustrates a simplified version of the quartz crystal along with its impedance equation and pole zero pattern. Typical values of capacitance, inductance and resistance are, for example, $w_o = 10^7$ rad/sec, $C/C_o = .01$, $C_o = 4$pf and $Q_L = 20$k. These values lead to C = .04pf, L = 250mH and r = 125 . For this case, Δw, the vertical spacing between the pole and zero in the vicinity of w_o approximately equals $w_o/200$. While the negative real portion of the complex pole and zero is at a distance of $w_o/40{,}000$ from the jw axis. Thus, in effect, we have two isolated very high Q poles and zeros. With this in mind we see that the crystal can operate as a low impedance (near a zero) or as a high impedance (near a pole).

In the series resonant mode of operation the crystal is placed directly in the feedback path for the purpose of holding the loop gain below the minimum required for oscillation except at the series resonant frequency of the crystal. A capacitance C_x placed in series with the crystal can be used to modify the resonant frequency slightly. However, this slight adjustment is purchased at the expense of narrowing the pole-zero spacing.

Field effect transistor oscillators predominantly employ the crystal operating in the high impedance mode. The operating frequency tends to be below the pole of Z(s) by approximately w_o/Q_L or less. Within this rather narrow frequency range the crystal looks like a parallel inductance-resistance combination and as such the crystal is often used to replace an inductance in a Colpitts or Hartley oscillator configuration.

A relatively new method for constructing oscillators involves the use of surface acoustic wave devices (SAW).

The basic mode of energy transfer in SAW devices involves the propagation of elastic waves along the surface of a piezoelectric substrate. The propagation of elastic waves is typically in the range of 10^3 to 10^4m/sec. This surface wave excitation results in material deformation near the surface of the substrate. The actual material displacement has its greatest amplitude at the free surface and decays exponentially with depth into the solid. Essentially, all the mechanical energy transported by the wave is concentrated within one wavelength of the surface. When these elastic waves are introduced on a piezoelectric substrate, local electric fields are induced. The electric fields travel along with the mechanical

wave and extend into the space above the surface of the solid. Metal electrodes placed on the surface of the substrate will interact with these electrical fields. The resulting effect can then be used by connecting the electrodes to an external circuit.

Due to impedance requirements and size restrictions, surface wave electrodes or transducers have a limited dimension transverse to the direction of the exciting wave. Typically this dimension, which determines the width of the radiating wave, lies within the range of 10 to 100 wavelengths in magnitude. To a first order, simple interdigital transducers exhibit a two-dimensional diffraction analogous to the diffraction encountered in optics when a plane wave illuminates a long narrow slit.

For an elastic wave the end of the transducer is analogous to the slit width, that is, it determines the dimension of 2a. Just as in the optics case, two diffraction regions exist, a Fresnel region and a Fraunhofer region. In the Fresnel region, which extends from the aperture to approximately a^2/λ, the radiation of the wave is beamlike; while in the region beyond a^2/λ, the Fraunhofer region, the wave pattern has a constant angular form. Thus, if we wish to have the energy propagated between transducers as a more or less parallel beam, we must operate in the Fresnel region. By operating in the Fresnel region, almost all of the energy radiated by the transmitting transducer will be captured by the receiving transducer of aperture comparable to that of the transmitter. By contrast, operation in the Fraunhofer region will result in an appreciable loss of energy due to diffractive spreading of the input wave.

The two most common SAW oscillators are the SAW delay line oscillator and the SAW resonator oscillator. SAW oscillators have a stability which is considerably better than the common LC oscillator but not as good as the crystal controlled oscillator. SAW oscillators do not relay on harmonic operation as do some crystal oscillators. In fact, resonators at frequencies above one GHz with Q values over 3200 have been fabricated.

Basically, a SAW delay line oscillator consists of a SAW delay line and an external amplifier which provides positive feedback from the output transducer to the input transducer. The figure below illustrates the essence of such a circuit.

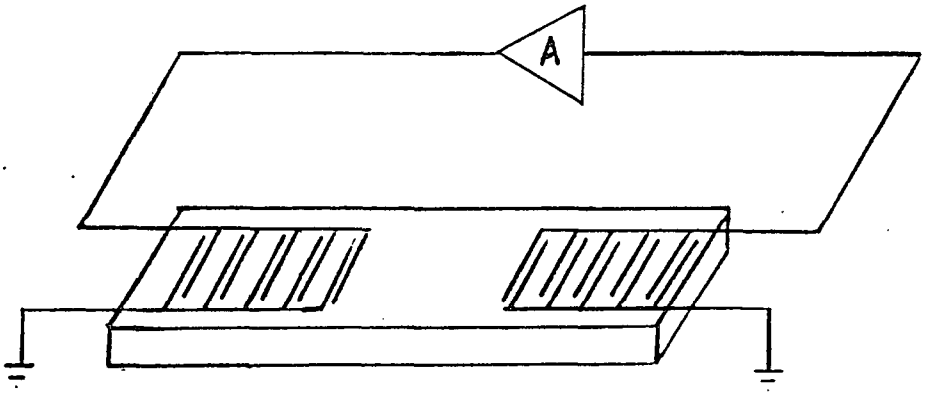

Figure 12. Delay Line Oscillator

The condition for oscillation is that the phase shift around the loop must be an integral multiple of 2π . Thus,

$$w_o L/V_r + \Phi_E = 2\pi N$$

where L = effective delay path

V_R = Rayleigh velocity of the surface wave

w_o = angular frequency of oscillation

ϕ_E = phase shift external to the delay line

If we assume that ϕ_E is a constant, then $\frac{dw_o}{w_o} = \frac{dV_R}{V_R} - \frac{dL}{L}$. Also, if we neglect the thermal expansion, we find that $\frac{dw_o}{w_o} = dV_R/V_R$. Considering the thermal expansion to be negligible is reasonable because the temperature coefficient of expansion is very small compared to that of the velocity. For example, the temperature coefficient of expansion for YZ $LiNbO_3$ is on the order of 2ppm/^oC while that of velocity is about 90ppm/^oC. Therefore, we see that frequency stability is primarily a function of the Rayleigh velocity. Stated in a slightly different manner, if we let the phase shift between the input and output transducer be given by

$$\phi = \int_o^L (w/V_R(z))dz$$

where z is the direction of propagation, and since temperature is taken to be a spatial function of depth only we find that V_R is independent of z and thus $\phi = wL/V_R$. Now if we assume w is the frequency of an externally connected frequency generator, thermal variations will cause overall changes in L and V_R. Thus, $\frac{d\phi}{\phi} = \frac{dL}{L} - \frac{dV_r}{V_r}$. By the same reasoning we applied above we find that $\frac{d\phi}{\phi} = \frac{-dV_r}{V_r}$. Therefore, the phase change is approximately of the same order as that of the Rayleigh velocity. A change in phase implies a change in w_o for oscillation to occur.

The second type of SAW device employed in the construction of oscillators is the SAW resonator. The resonator relies on the reflection from shallow reflecting groove arrays etched into the surface of the substrate. The figure below illustrates the basic construction of a SAW

resonator and resonator controlled oscillator.

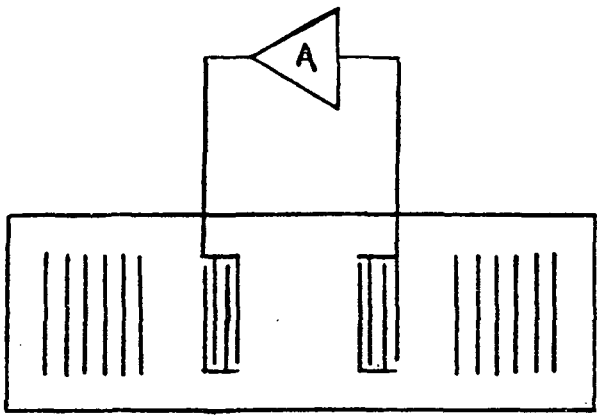

Figure 13. SAW Resonator Oscillator

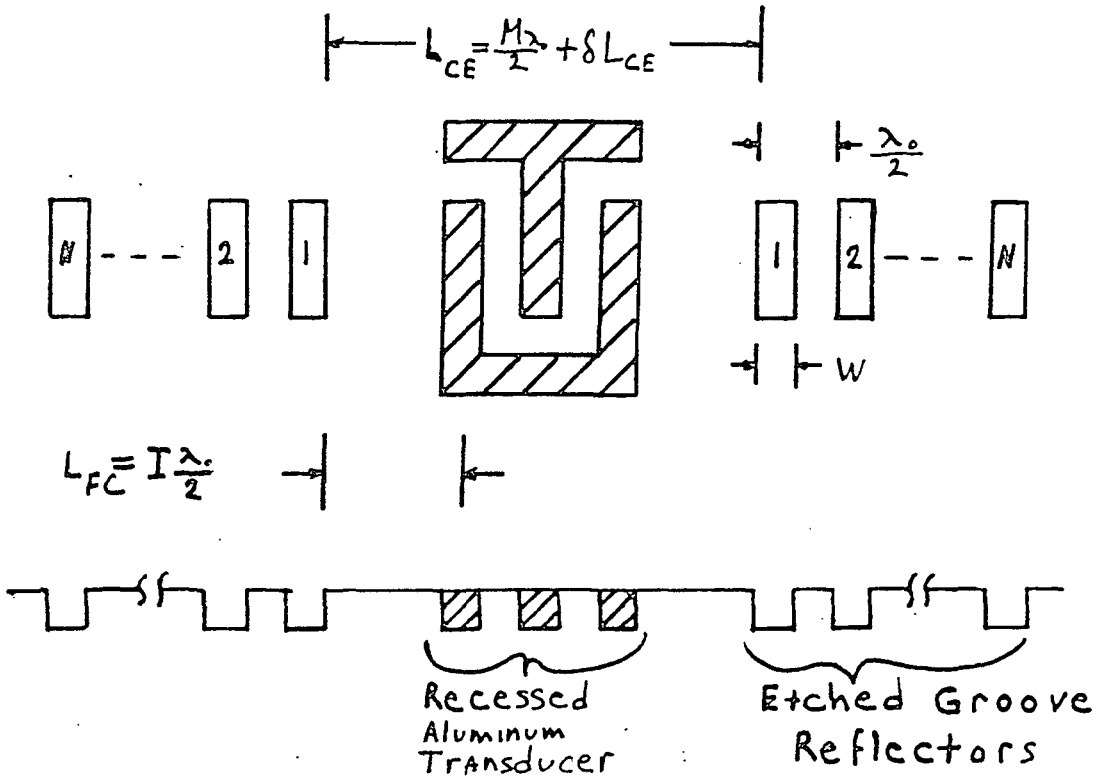

Figure 14. One-Port SAW Resonator

The reflectors, consisting of arrays of shallow etched grooves are spaced to form a resonant cavity in which one or two recessed aluminum transducers are located. Maximization of the cavity length is essential to achieve high Q values. Also, the recessed-transducer configuration virtually eliminates transducer reflections and the distortion resulting from this source. When the resonance is not centered in the reflector stopband, loss and distortion increase dramatically. This undesireable effect results because radiation losses are not minimized and resonance develops asymmetrically.

The presence of a transducer within the resonant cavity will contribute to losses due to finite electrode conductivity and from bulk mode scattering associated with surface wave scattering for acoustically reflecting electrodes. Distortion will be introduced by the transducers due to acoustic reflection and by the velocity differences between the transducer, the free surface and the reflector sections of the resonator. A thorough discussion on how these effects interrelate can be found in [2]. In this discussion it is shown that the recessed metal transducer on quartz reduces losses and distortion in resonators.

The portion of the resonator which serves to contain the energy in the resonant cavity is made up of the surface wave reflectors. Their ability to contain the energy is by no means perfect. Loss of energy does occur through radiation transmitted through the reflector and by scattering energy in the bulk acoustic modes.

The operational characteristics of an etched groove reflector are primarily determined by the groove depth (h), the total number of grooves (N) in an array, and the separation of the grooves ($\lambda_o/2$). Secondary factors are the groove profile and the groove width to separation ratio ($2W/\lambda_o$). Groove profile has been shown, theoretically at least, to be noncritical by Otto and Gerard [3]. The effect of the groove width to separation ratio has been shown by Li, Alosow and Williamson [4] to result in a maximum reflectivity when $2W/\lambda_o$ is slightly less than 0.5 depending on the groove depth.

Bulk acoustic mode losses (L_{BG}) occur whenever a surface wave is reflected from a discontinuity. These losses increase with the size of the discontinuity where L_{BG} is directly proportional to $(h/\lambda_o)^2$, [5]. Thus, in order to reduce L_{BG}, groove depth is reduced. However, if each groove is shallow and lightly reflecting, there must be a large number of grooves in order to obtain sufficiently low radiation loss. In the lower frequency range between 10MHz and 300MHz, the material losses are fairly low, and thus extremely shallow grooves ($h/\lambda_o \leq 0.5\%$) may be necessary to attain the desired high Q value. This would dictate very long arrays, and thereby the overall device dimensions may be the limiting factor. At significantly higher frequencies ($F < 800MHz$) material losses increase considerably and as such, allow for somewhat deeper grooves ($h/\lambda_o \geq 2\%$ perhaps) and still keep the bulk-mode losses less than losses due to the material. A more detailed discussion on reflector construction is given by Tanski [2].

The recessed transducer/grooved-relector system lends itself to a simple fabrication process. It is necessary in resonator fabrication that no critical photolithograph mask realignment be performed since each of the device components (reflectors and transducer) must be positioned to an accuracy of a few hundredths of a wavelength or better with respect to one another. This accuracy cannot generally be attained by using conventional methods to superimpose masking steps. A complete discussion of the fabrication process steps is given by Tanski [2].

Application of the techniques mentioned above has resulted in the production of resonators with a series resonant Q of 75300 and F_c of 72MHz ($V_F \approx 3158$ m/sec). This device had an 80-λ_o cavity, $\lambda_o = 44$ microns. The reflectors, etched to $h/\lambda_o = 1\%$, contained in excess of 1000 grooves.

Experiments

In the initial stages of this experiment experience was gained in the construction and operation of conventional oscillators. The oscillator circuit used is shown below.

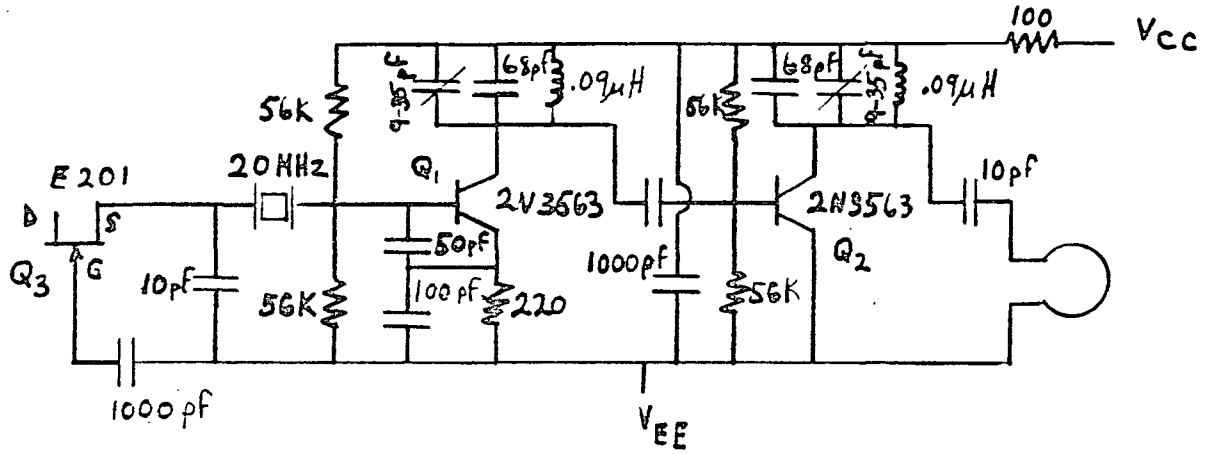

Figure 15. Two Stage Oscillator-Filter-Amplifier Circuit

This circuit utilized the clapp oscillator configuration and two tuned stages to filter off the desired harmonic component. The crystal used had a fundamental frequency of 20MHz. Each stage was tuned to the third harmonic or 60MHz. The air core inductors had a calculated inductance of 0.09uH and a measured Q_c of 147 at 50MHz. The tank circuits were tuned by adjusting a 4-35pf variable capacitor, in parallel with a 68pf capacitor, until the 60MHz frequency component was maximized. The supply voltages V_{CC} and V_{EE} were set at 2.0 volts and -2.0 volts respectively.

The harmonic frequency components at various points in the oscillator circuit were measured with a Hewlett-Packard 8557A Spectrum Analyzer. The following data was obtained.

Measurement Point	Frequency Component	Magnitude
Drain of Q_3	20MHz	-19dB
	40MHz	-42dB
	60MHz	-34dB
Collector of Q_1	20MHz	-31dB
	40MHz	-17dB
	60MHz	-11dB
Collector of Q2	20MHz	-34dB
	40MHz	-25dB
	60MHz	6dB

TABLE 1: Harmonic Amplitudes

Thus, we can see that the 60MHz component has been increased in magnitude by a factor of 100 while the 20MHz and 40MHz components have been altered by factors of .18 and 7.1 respectively. Also, at the output of the second stage the 60MHz component overpowers the 20MHz component by 100:1 and overpowers the 40MHz component by 35.5:1. The output of the second stage exhibited a relatively good sinusoidal symmetry and an RMS voltage of 113mV. The 20MHz input to Q_1 had an RMS voltage of 18.5mV. This technique of amplification and filtering can be applied up to the fifth harmonic of the fundamental frequency of each stage, provided we stay within the frequency limit of the transistor employed.

In an effort to better understand the input-output characteristics of a surface acoustic wave (SAW) device, the filtering behavior of a crystal technology CTI 55B SAW filter was tested.

The CTI 55B SAW filter is designed for use as an output filter for Class 1 channel 3 and channel 4 signal sources for direct coupling to the antenna terminals of a color TV receiver. The illustration below outlines the pin layout and connections used.

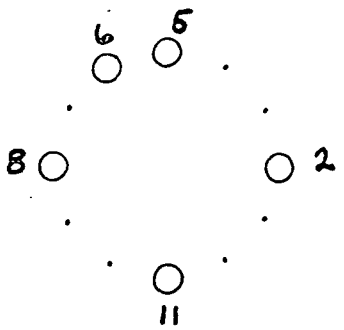

Pin Connections

Pin 2	NC
5	Input Channel 3
6	Ground
8	Input Channel 4
11	Output

Figure 16. CTI 55B Pin Layout

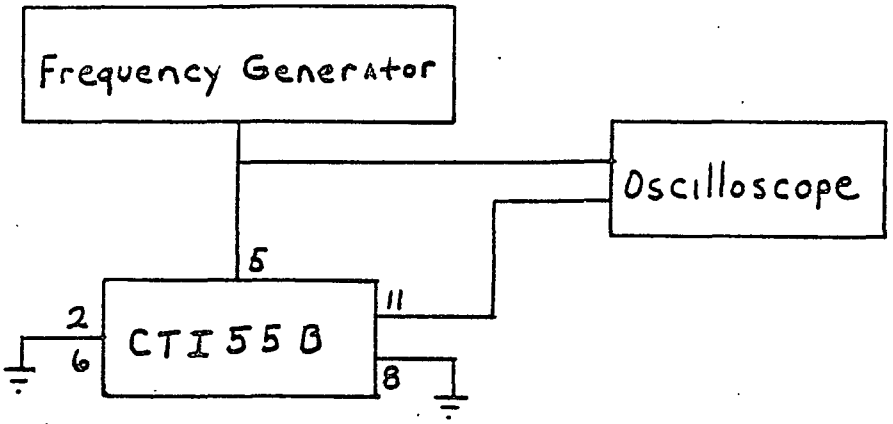

Figure 17. Test Circuit

The channel 3 input (pin 5) has an RF impedance of 50-j140 ohms at 61.25MHz. However, no attempt was made to match this impedance during testing. For testing purposes the CTI 55B was mounted and grounded inside a metal box with male BNC connectors on each end. Input and output signals were transmitted through RG-58 coaxial cable throughout the test circuit. Table 2 and Figure 21 below detail the data generated.

Frequency (MHz)	Input (Vp-p)	Output (Vp-p)	Insertion Loss (dB)
50	24.0	0.25	-39.6
52	20.0	0.32	-35.9
54	16.8	0.34	-33.9
56	14.5	0.46	-30.0
58	13.0	0.64	-26.2
60	11.5	0.38	-29.6
62	10.8	3.6	-9.5
64	11.0	4.6	-7.6
66	10.8	4.7	-7.2
68	12.5	.85	-23.3
70	13.0	1.05	-21.9
72	14.8	1.10	-22.6
74	14.8	.98	-23.6
76	12.0	.85	-23.0
78	9.0	.60	-23.5
80	12.0	.78	-23.7

TABLE 2: In-Band Response of CTI 55B

This data coincided well with the data provided on the CTI 55B data sheet. However, the CTI 55B data sheet showed an insertion loss of 10dB less throughout the in-band as compared to the data presented here. With consideration for the test method used in this experiement, a difference of 10dB is acceptable.

A SAW resonator was fabricated for the purpose of constructing a SAW oscillator. The reflector array grooves were spaced approximately 18μm apart in order to realize a resonator in the 80MHz range. The resonator layout is shown in Figure 18.

Tests conducted to determine the attenuation in the resonant cavity found that an attenuation of approximately -69.5dB resulted from propagation through the cavity. Figure 19 illustrates this attenuation. The upper pulse represents the signal sent down the resonant cavity. The lower trace represents the signal picked up by the resonator transducer

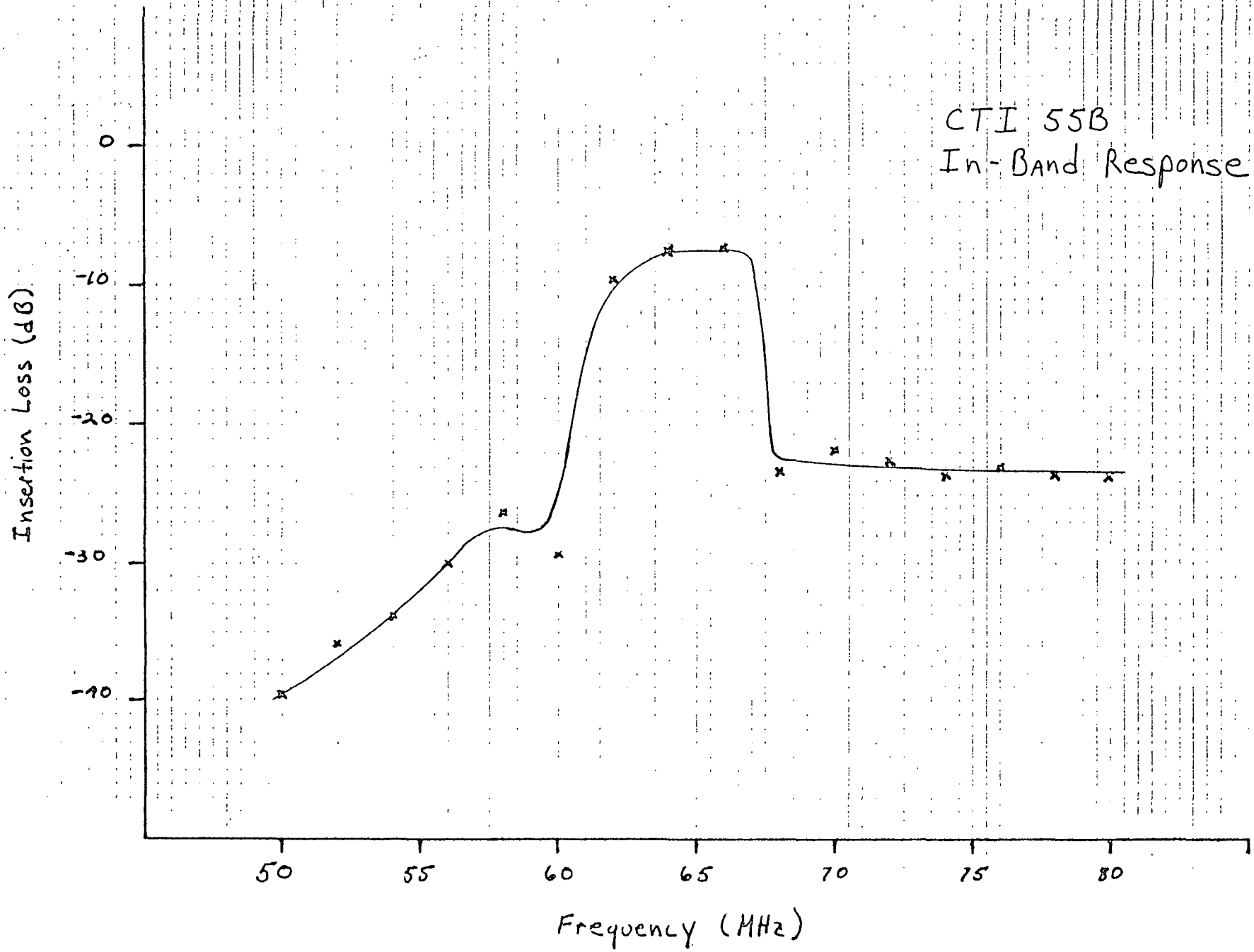
CTI 55B
In-Band Response
Insertion Loss (dB)
0
-10
-20
-30
-40
50
55
60
65
70
75
80
Frequency (MHz)

Figure 21

at the launch port. Note the spike at approximately 450nsec after the input pulse was launched.

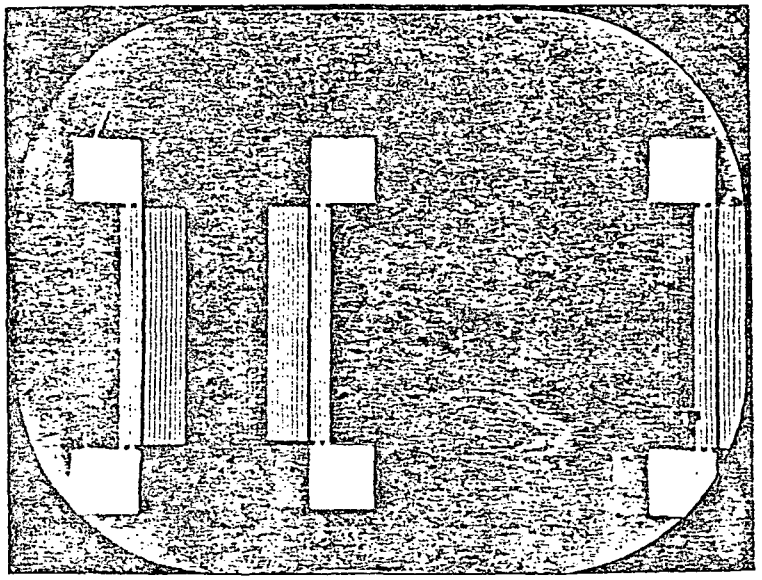

Figure 18. Two-port SAW Resonator Layout

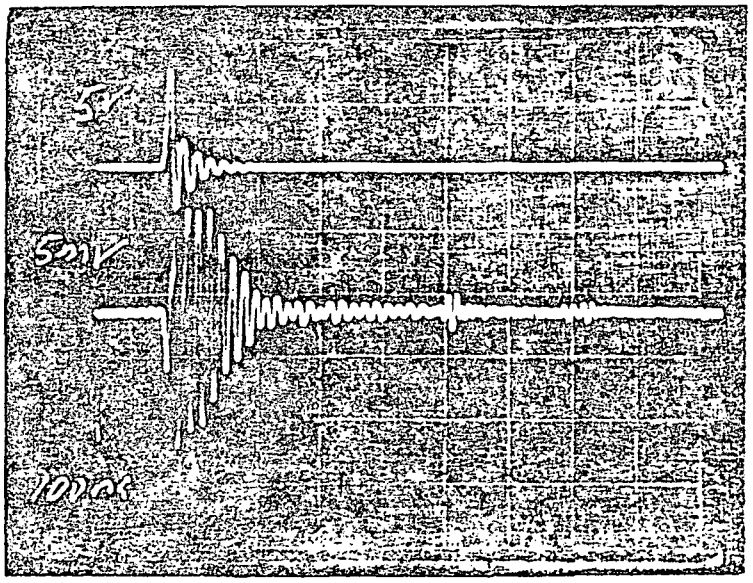

Figure 19. Resonator Pulse Response

The magnitude of this spike represents the degree of attenuation due to the absorbtion of energy within the resonant cavity and losses associated with the reflecting array grooves. This test indicates that an external amplifier with a gain of approximately 70dB will be necessary to sustain oscillations.

The circuit shown below was designed for the purpose of providing the necessary external gain to allow sustained SAW resonator oscillation.

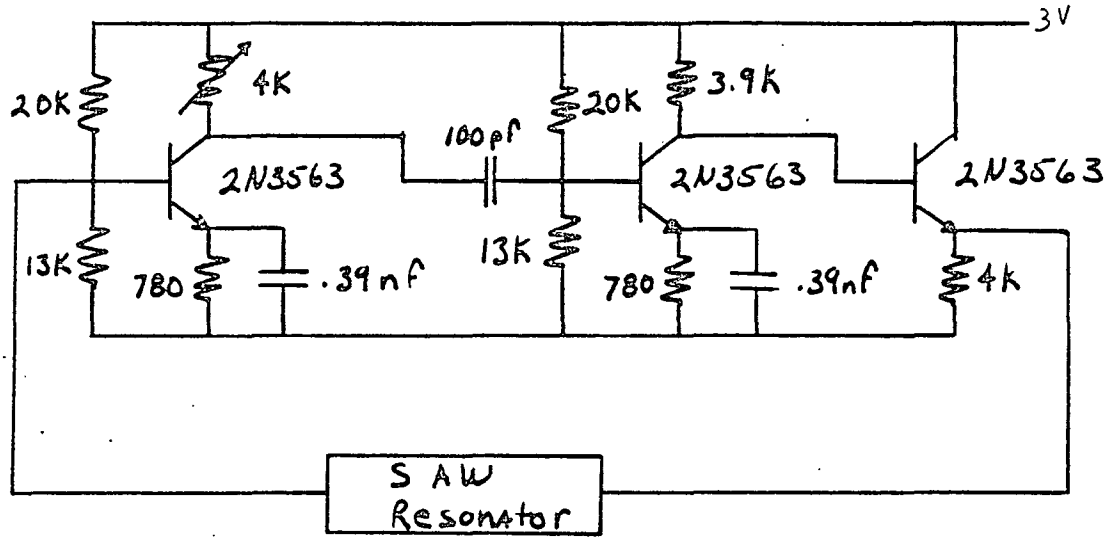

Figure 20. SAW Resonator-Oscillator Circuit

The two-stage amplifier has a maximum theoretical gain of about 75dB. At the time of this report, however, sustained oscillations have not been achieved.

Summary

This paper dealt with the application of SAW resonators in the construction of oscillator circuits. While the construction of a stable oscillator was not achieved, suggestions for future improvement are outlined below.

1. Decrease the resonant cavity width. This should reduce the loss of energy due to substrate material absorption.
2. Attempt to optimize the grooved reflector depth. This will reduce distortion and provide more efficient reflection of energy into the resonant cavity.
3. Increase the number of reflectors in the reflector arrays. This will result in more energy being reflected into the resonant cavity.
4. Design a more sophisticated amplifier which can achieve the required high gain-bandwidth products which are necessary to achieve stable oscillations with the present SAW resonator.

Acknowledgement

The author would like to thank Dr. Udo Strasilla for his helpful suggestions throughout this work and Dr. Chen Yuen for fabricating the SAW resonator.

References

1. K. Clark and D. Hess, Communication Circuits: Analysis and Design, Addison-Wesley Publishing Company, Reading, Massachusetts, 1978.

2. W. Tanski,"Surface Acoustic Wave Resonators on Quartz" IEEE Transactions on Sonics and Ultrasonics, Vol. 50-26, March 1979.

3. O. W. Otto and H. M. Gerard, "On Rayleigh wave reflection from grooves at oblique incidence and an emperical method for bulk wave scattering in RAC devices," Proc. 1977, Ultrasonics Symposium, pp. 596-601 (IEEE Cat No. 77, CH 1264-150)

4. R. C. M. Li, J.A. Alusow, and R. C. Williamson, "Experimental exploration of the limits of achieveable Q of grooved surface-wave resonators, Proc. 1975, Ultrasonics Symposium, pp. 279-283 (IEEE Cat No. 75 CHO 994-4SU)

5. J. P. Parekh and H.S. Tuan, "Effect of groove-depth variation on the performance of uniform SAW grooved reflector arrays," Appl. Phys. Letters, Vol. 32, pp. 787-789, 1978.

6. R. Dobson, "An Introduction to the Design of Surface Acoustic Wave Devices," Defence Research Centre, Salisbury, South Australia, Technical Report AEL-001-TR, April 1978.

7. D. L. Schilling and C. Belove, Electronic Circuits: Discrete and Integrated, McGraw-Hill Book Company, New York, New York 1979.

8. Model CTI 55B SAW Output Modulation Filter Data Sheet, Crystal Technology, Inc., Palo Alto, California.

9. K. H. Dinh, "Response of Surface Acoustic Wave Devices to High-Speed Thermal Radiation," IEEE Transactions on Sonics and Ultrasonics, March 1979.

Simulating a SAW Oscillator Using a Lumped Element LC Delay Line

Presented to

Professor Udo Strasilla

In Partial Fulfillment of
the Requirements for the Completion
of E.E. 180

BY

Timothy C. Upshaw

San Jose State University
San Jose , California

December 6, 1981

TABLE OF CONTENTS

LIST OF FIGURES AND TABLES

ACKNOWLEDGMENTS

The author would like to thank Prof. Udo Strasilla for his help and guidance throughout this work. My gratitude goes to him for his overall knowledge of the subject of SAW devices which afforded me to absorb invaluable and practical information.

ABSTRACT

The Lumped element(LC) delay line is analogous to the SAW(Surface-Acoustic-Wave) device because they both have the ability to delay the signal. This paper analyzes an oscillator constructed from a lumped element delay line to compare with the SAW oscillator. The LC oscillator is frequency variable (depending on the delay tap) and contains only two elements: the LC delay line and a Nand gate. This paper describes delay line theory, analyzes the delay line oscillator, and discusses the SAW device as an oscillator.

1.0 INTRODUCTION

The purpose of this paper is to investigate the characteristics of Delay Lines used as oscillators. In an experimental set-up, these characteristics will be measured, discussed and analyzed. Other oscillator alternatives that will improve the Delay Line oscillator's performance will be discussed also: The ECL Delay Line oscillator and the Tunnel Diode Delay Line oscillator.

Finally, the Delay Line oscillator will be compared to the SAW oscillator.

2.0 BACKGROUND INFORMATION

2.1 Electromagnetic Delay Line

The Electromagnetic Delay Line is merely a "compressed" form of a conventional transmission line and exhibits the same general electrical properties. The many advantages and innumerable uses of such lines have been a tremendous boom to the electronic industry for some of the reasons given below:

1. Delay capabilities from nanoseconds to milliseconds.
2. Ability to temporarily store many "bits" of infomation using pulses.
3. Low-Loss Passive devices require no power(other than the input signal) and which are very stable with time and temperature.
4. They are useful as energy storage devices.

The information can be digital or analog. In digital applications, we are interested in the pulse fidelity reproduction at the output of the delay line. In analog applications, we are interested in the phase-linearity produced by the delay line.

Of all the types of delay lines available, the electromagnetic delay line is the most widely used and fits the most applications due to its wide band response. (See Figure 1)

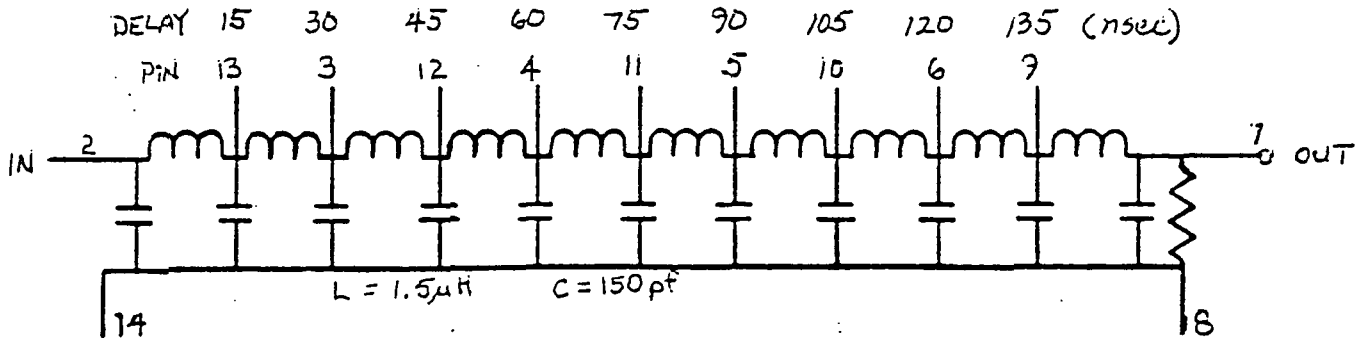

Figure 1 Ten Section Delay Line

2.2 General Delay Line Calculations

ABBREVIATIONS

n	Number of Taps
T_d	Time Delay, Sec. (variable)
T_r	Time Rise, Sec. (= 25 nsec)
Z_o	Characteristic Impedance (= 100 ohms)
BW	Bandwidth @ 3 dB down point (= 14 Mhz)

1. CAPACITANCE $C = T_d/Z_o = 15 \text{ nsec}/100 = \underline{150 \text{ pf}}$

2. INDUCTANCE $L = T_d x Z_o = 15 \text{ nsec} x 100 = \underline{1.5 \text{ uH}}$

3. QUALITY FACTOR $Q = T_d/T_r = 150 \text{ nsec}/25 \text{ nsec} = \underline{6}$
   (Note that the <u>total</u> delay of the delay line is used here.)

4. RESULT OF MISMATCHING E TERMINATION $= \dfrac{E \text{ Initial}}{Z_o/2R_t + .5}$
   where R_t is the terminating resistance.

2.3 Circuit Operation

To make an oscillator from a delay line, a Nand Gate was used to generate the pulses. (See Figure 2) To start oscillation, pin 1 of the gate is tied high to +5 volts. Assuming that pin 2 of the gate is low at the present state, this results in a logical high at the gate's output. The logical high goes through the delay and exits to pin 2 of the Nand gate. This cycle reoccurs thereby initiating oscillation. Measurements were taken from various taps of the delay line which produced different frequencies. (Discussed in Section 3.0)

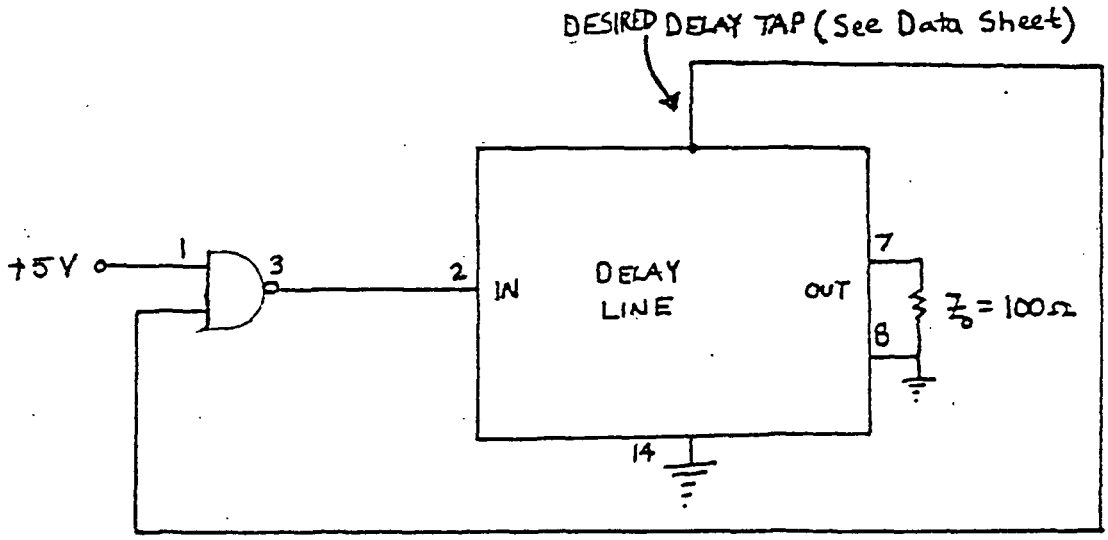

Figure 2 Experimental Circuit Setup

DATA SHEET

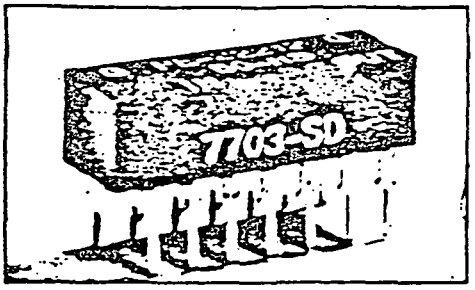

Pulse Engineering Inc.

A VARIAN SUBSIDIARY

ELECTRICAL SPECIFICATIONS AT 25°C

Catalog Number	Impedance Zo Ohms ±10%	Total Delay ns ±5%	Delay Per Tap (ns)	Rise Time ns Max.	DCR Ohms Max.	Distortion At Taps % Max.	Schematic
22212	100	50	5 ±2.0	8.0	2.3	10	A
22213	100	100	10 ±2.0	15.0	3.0	10	A
22214	100	150	15 ±3.0	25.0	3.6	10	A
22215	100	200	20 ±3.0	30.0	4.5	10	A
22216	200	50	5 ±2.0	8.0	2.6	10	A
22217	200	100	10 ±2.0	15.0	3.6	10	A
22218	200	150	15 ±3.0	24.0	4.5	10	A
22219	200	200	20 ±3.0	30.0	5.0	10	A
22220	200	300	30 ±3.0	45.0	8.0	10	A
22223	100	50	5 ±2.0	8.0	2.3	10	B
22224	100	100	10 ±2.0	15.0	3.0	10	B
22225	100	150	15 ±3.0	23.0	3.6	10	B
22226	100	200	20 ±3.0	30.0	4.5	10	B
22227	200	50	5 ±2.0	8.0	2.6	10	B
22228	200	100	10 ±2.0	15.0	3.6	10	B
22229	200	150	15 ±3.0	24.0	4.5	10	B
22230	200	200	20 ±3.0	30.0	5.0	10	B
22231	200	300	30 ±3.0	45.0	8.0	10	B

Data Subject To Change Without Notice

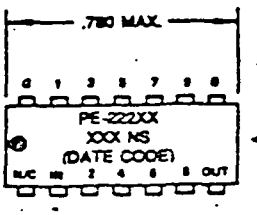

Figure A

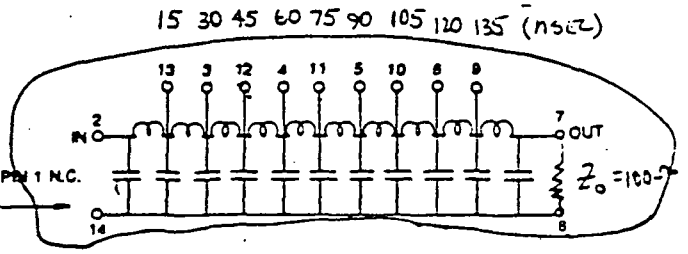

3.0 PROCEDURE

The circuit was constructed as shown in Figure 2. In an attempt to avoid unwanted ground loops and their associated problems, the DC power supply and the oscilloscope had their ground leads brought to the same common ground point.

To obtain the desired delay of the delay line, the jumper wire was connected from pin 2 of the Nand Gate to the desired tap of the delay line. The DC voltage was set at 5 volts. On the oscilloscope(Trigger source, mode and slope on EXT.,AUTO and + respectively), the waveforms of e_{in} and e_d(delayed signal) were observed.(See Figure 3)

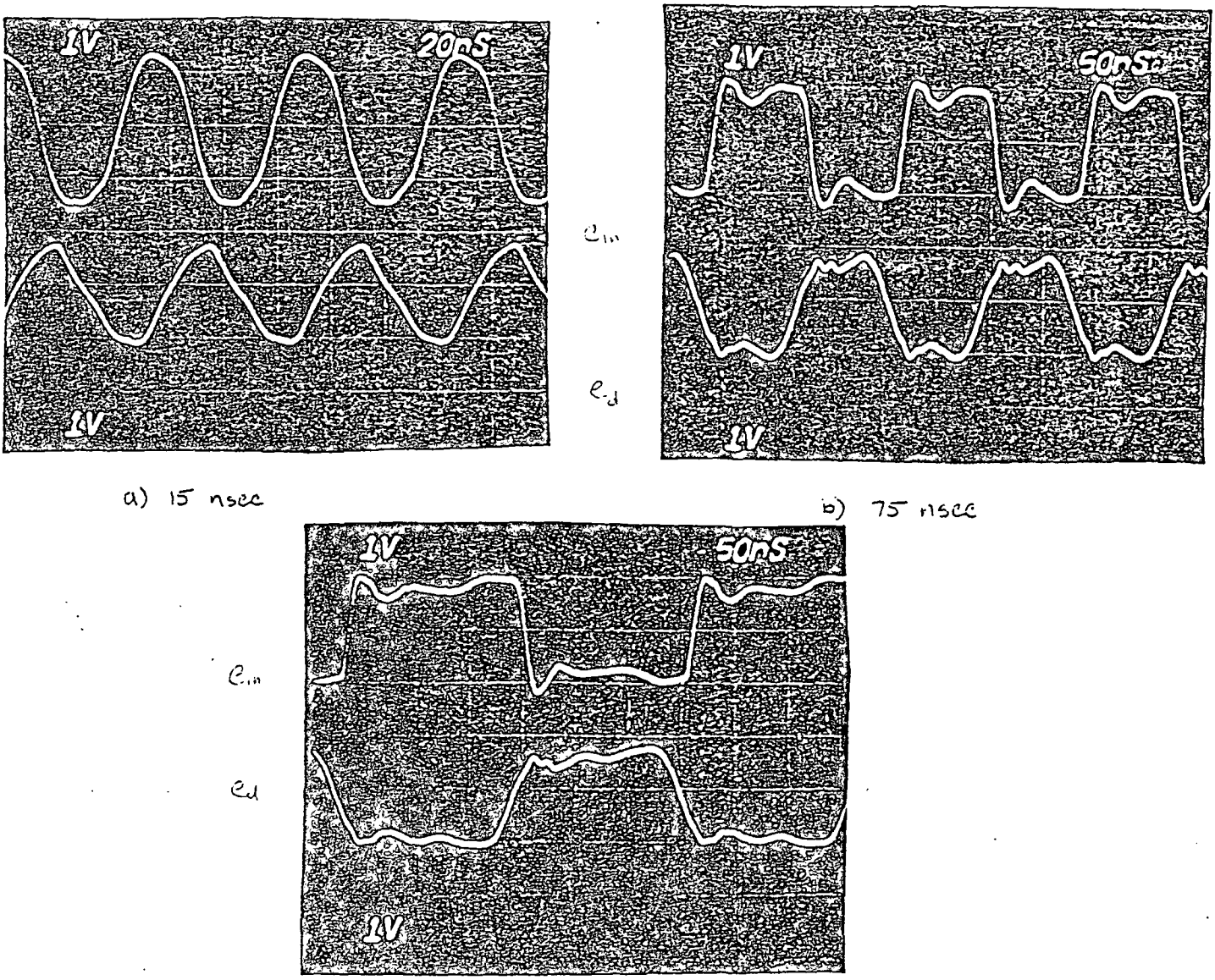

Figure 3

EQUIPMENT LIST

1. DC Power Supply
2. Oscilloscope (Tektronix 475)
3. Pulse Engineering LC Delay Line
4. 74LS00 Dual Input Nand Gate
5. 2"x2" Perf Board
6. 100 ohm resistor
7. Wire Wrap wire
8. Jumper wire
9. Chip clip

3.1 Frequency Measurements

To obtain the 15 nsec delay, the jumper wire was connected from pin 2 of the Nand Gate to pin 13 of the delay line. The waveform in Figure 3a was observed and the corresponding frequency measurement is:

T(period) = 3 div x 20 nsec/div = 60 nsec

f = 1/T = 16.67 Mhz

Measurements were recorded for the 75 and 150 nsec taps and placed in Table 1.

TABLE 1

Delay(nsec)	Period(nsec)	Frequency(Mhz)
15	60	16.67
75	180	5.55
150	320	3.12

3.2 Phase Measurements

The phase difference of e_{in} and e_d was measured in this procedure. From an identifiable point on the waveform, the phase shift was measure by the following procedure: The distance(in divisions) of one period of this signal represents 360°. The result of the shift in divisions divided by the period in divisions is multiplied by 360° to obtain the phase shift between the two signals in degrees. The results are in Table 2.

TABLE 2

Delay(nsec)	Shift(div)	Period(div)	Phase Shift(deg)
15	0.8	2.9	99.3
75	1.5	3.6	150
150	3.2	6.4	180

3.3 Voltage Measurements

In this step, the peak-to-peak voltages were measured and recorded in Table 3. Note that the attenuation increases as the frequency increases.

TABLE 3

Delay (nsec)	Frequency (Mhz)	e_{in} (V)	e_d (V)	Attenuation (dB)
15	16.67	2.8	1.8	-3.81
75	5.55	2.2	1.9	-1.27
150	3.12	2.0	1.9	-0.9

3.4 Mismatched Termination

Out of curiosity, the termination impedance was removed from the circuit. As Z_o went to infinity, the amplitude of the delayed signal, e_d increased twofold! The output of the 150 nsec delay was severely distorted when Z_o was removed. (See Figure 4)

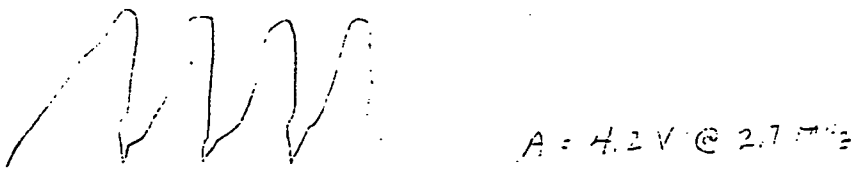

Figure 4 e_d with Z_o removed

The cause of this effect will be discussed in Section 4.1.

4.0 DISCUSSION OF RESULTS

4.1 Analysis of Waveform Shapes

Referring to Figure 3, it is apparent that the waveform is almost a square wave at the 150 nsec tap and almost sinusoidal at the 15 nsec tap. This is related to the rise time and switching limitations of the Nand Gate. In the 15 nsec case, the circuit is oscillating at a rate which is too fast for the speed of the Nand Gate. The 74LS00 has a worst case rise and fall time of 15 nsec each. The gate does not have adequate time for the pulse to properly settle into a square wave, therefore the corners are rounded off and the result is an approximate sine wave. In the 150 nsec case, this speed is slow enough for the Nand Gate to handle, so the result is a square wave.

In the experiment, the amplitude increased twofold when the termination impedance was removed. If the improper termination is used, a signal reflection will result as shown in Figure 5.

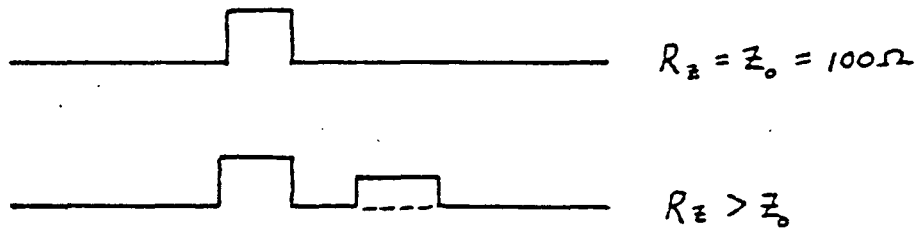

Figure 5 Improper Termination

Reflections such as termination mismatch is undesirable since this will result in distortion in the input and output signal. Voltage gain due to improper mismatch at the output is expressed in Section 2.3.

$$E_t = \frac{E_i}{Z_o/2R_t + .5}$$

Where E_t = Voltage at Termination

E_i = Voltage at input

R_t = Terminating value of resistor

In this case, assume E_i = 1 volt. When R_t = infinity then,

$$E_t = \frac{1\ V}{100/2(\infty)+.5} = \frac{1\ V}{.5} = \underline{2V}$$

0

This shows that the voltage doubles for an infinite termination impedance.

4.2 Attenuation and Filtering Effects

Figure 6 shows one section of the delay line.

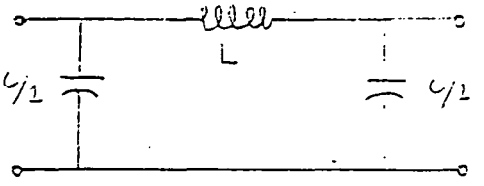

Figure 6

Its frequency response is shown in Figure 7.

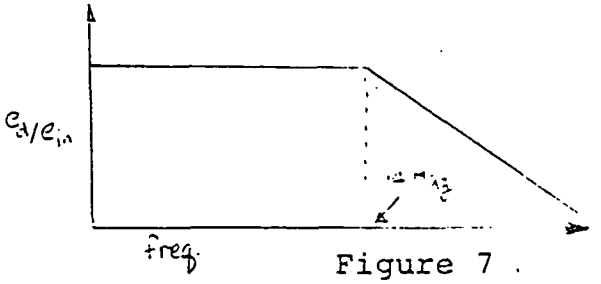

Figure 7

Figure 6 is a "constant k" low pass filter. It is value of the L's and C's that determine the cutoff frequency of the delay line per unit length. It has an approximate bandwidth of 14 Mhz. This is the reason why the delayed signal becomes attenuated as the frequency increases. At lower frequencies, the 150 nsec tap, attenuation approaches zero.

Attenuation in a delay line may be the effect of several sources of loss:

1. Internal DC resistance of the delay line
2. Dielectric and ground plane losses
3. Pulse Width limitations

4.3 Frequency Response

The frequency response is a function of the number of sections into which L and C are divided. A larger number of sections will reduce L and C of each section thereby increasing the overall frequency response. Since most delay line inputs are composed of a fundamental and odd harmonics, the frequency components must be delayed equally to assure minimum pulse shape distortion.

If the higher frequencies of the incoming pulse are delayed to a greater extent than the lower frequencies, then the output pulse of the delay line will appear as in Figure 8a. If the higher frequencies are delayed less than the lower ones, then the output will appear as in Figure 8b.

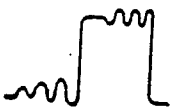

Figure 8a

Figure 8b

The frequency response of a delay line affects its ability to approach the rise time of the input pulse to be delayed. Therefore, frequency response is accounted for in rise time of the delay line.

4.4 Phase Shift

Since the signal coming out of a delay line is delayed in time, it is clear that there is also a phase shift of the delayed signal. Phase shift in a delay line is given by the followinf formula:

$$\text{Phase Shift(deg)} = T_d\text{(nsec)} \times \text{frequency} \times 360°$$

Table 4 shows theoretical and experimental phase shift obtained by using the above formula.

TABLE 4

T_d (nsec)	Frequency (Mhz)	Phase Shift (theo.)	Phase Shift (exp.)	Δ%
15	16.67	90°	99.3°	10.33
75	5.55	150°	150°	0
150	3.12	168.5°	180°	6.8

The error occurring between the theoretical calculations and the experimental values is probably due to human error in measuring the frequency of operation and the divisions for the phase shift measurements.

4.5 Frequency of Operation

The delay line oscillator has 10 taps which vary in delay time. For each tap, there is an associated frequency. To correlate the frequency with the delay time, we must add all of the delays in the signal path:

1. Delay time = variable
2. Rise time of delay line (T_r) = 25 nsec
3. Propagation delay times of the Nand gate.
   a) t_{pHL} (propagation delay from High to Low) =9.5 nsec(typ)
   b) t_{pLH} (propagation delay from Low to High) =9.5 nsec(typ)

For example, for the 15 nsec tap we get:

delay time	15 nsec
T_r	25 nsec
t_{pHL}	9.5 nsec
+ t_{pLH}	9.5 nsec
	59 nsec total (period)

frequency = 1/T = 16.9 Mhz

The actual frequency was 16.67 Mhz. The error percentage was: $\Delta\% = 1.7\%$.

5.0 DELAY LINE OSCILLATOR ALTERNATIVES

5.1 ECL Delay Line Oscillator

Other oscillator alternatives were considered for the delay line. One idea was to see if the frequency of operation would increase if an ECL Nand Gate was used. It has a lower propagation delay time than TTL. (approx. 2.7 nsec) The circuit was constructed as in Figure 9. The operation is the same as the TTL gate oscillator.

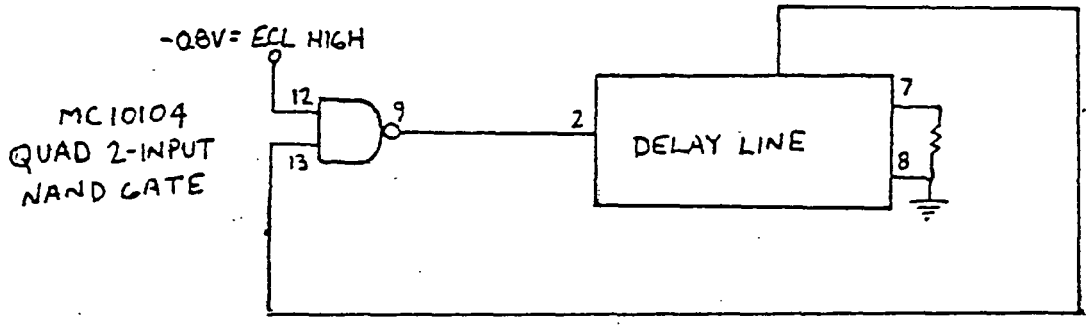

Figure 9 ECL Oscillator

This oscillator exhibited a frequency of 22 Mhz compared to the TTL's oscillator's 16.67 Mhz. (For the 15 nsec delay) This is a frequency increase of 32%, but due to this frequency, the output signal was attenuated more because the operation frequency exceeded the delay line's 14 Mhz bandwidth. The signal was attenuated by -4.7 dB.

5.2 Tunnel Diode Delay Line Oscillator

This circuit works as follows: When the diode switches from its low voltage state to its high voltage state, a voltage step occurs. The step is reflected back in opposite polarity after it propagates down the delay line by the short circuit. The diode reverses state when the reflected step is returned, thus generating a pulse train. The frequency rate of the signal is dependent on the time constant of the diode and the delay tap that is chosen. (See Figure 10)

This circuit did not work! Either the wrong diode was used by mistake or maybe it was defective.Time limitations did not permit further investigation.

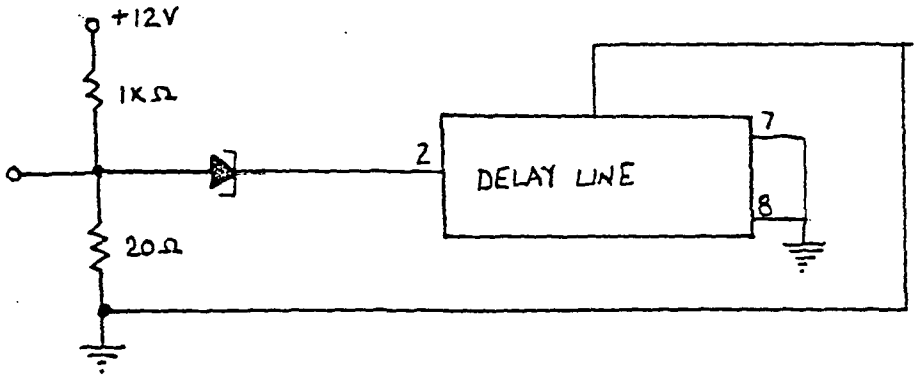

Figure 10 Tunnel Diode Oscillator

6.0 DELAY LINE COMPARISON WITH THE SAW DEVICE

Although my experience with the SAW device is limited, I can attempt to compare the Delay Line Oscillator to the SAW oscillator.

The unique feature about the TTL delay line oscillator discussed in this paper is the fact that it requires no external amplification to generate a signal. The TTL gate plays the main part in generating the signal. On the other hand, the SAW device's output is fed back to the input with sufficient gain to overcome the loss in the acoustic line. (See Figure 11)

The phase condition for the SAW device is

$$2\pi n = \phi_{el} + 2\pi f_n L/s$$

where n = integer

ϕ_{el} = phase shift through feedback loop

f_n = frequency of the n^{th} mode

L = acoustic path length

s = speed of sound

The frequency of oscillation is dependent to the relitive size of the phase shift and $2\pi f_n L/s$. The previous statement is an important property of the oscillator because it allows a choice to be made between modulation and stability capability.

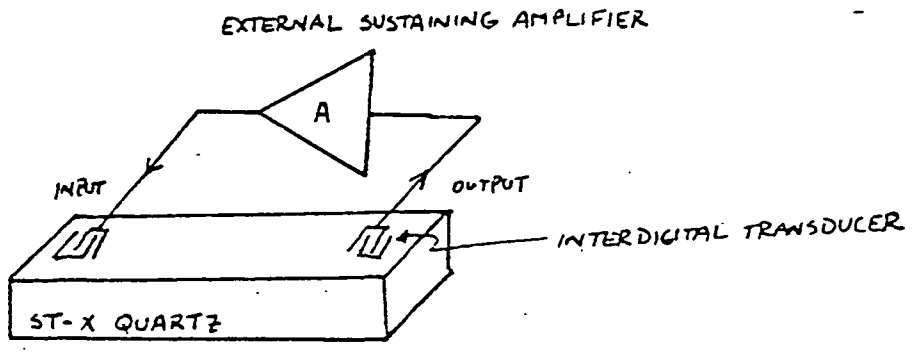

Figure 11 SAW Oscillator

The SAW oscillator depends on reflections from periodic discontinuities placed at half wavelength spacings to create a resonant structure. The LC Delay Line oscillator depends on transitions within the Nand Gate to generate pulses for oscillation.

This SAW oscillator will have a much better stability than the Delay Line oscillator. The Delay Line oscillator's frequency can be affected by temperature which affects the Nand Gate's operation. The SAW oscillator's frequency of operation will be much higher because it does not depend on the rise times and propagation delays as the Delay Line oscillator does. These extra delays slow down its frequency of operation considerably.

7.0 SAW DEVICE OSCILLATOR ATTEMPT

An attempt was made to construct a working SAW oscillator. For the sustaining external amplifier, the Harris HA-2535 was chosen because of its 320v/nsec slew rate. An estimated gain of about 60 dB(1000) is needed to overcome the attenuation of the delay line. The gain for closed loop operation was quickly calculated as follows:

$$G = \frac{-A}{1+AF} \quad \frac{R_f}{R_1+R_f} = -952 \cong -60\ dB$$

(SIGNAL IS TO BE INVERTED)

where $F = \frac{R_1}{R_1 + R_f} = \frac{500\Omega}{500 + 10M\Omega} = 5 \times 10^{-5}$

and $A = 1000$

The SAW device's pinout is shown in Figure 12.

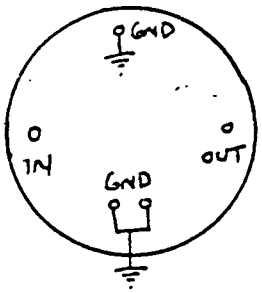

Figure 12 SAW device pinout

The circuit was constructed as shown in Figure 13.

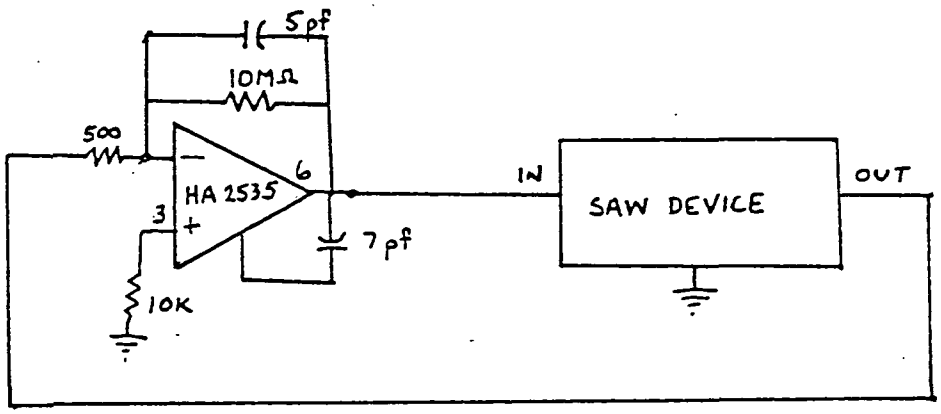

Figure 13 Saw oscillator

This circuit did not work also. Since the SAW device's attenuation is practically unknown, this may be a major factor in the oscillator's failure. The attenuation might be greater than 60 dB, which is the gain that corresponds to the op-amp's external components' values. Another possible reason for the failure may be due to a miscalculation for the op-amp's external components.(frequency compensation) If the op-amp is defective,the circuit will not operate. The SAW device, which was manufactured at San Jose State University could have been defective also.

8.0 CONCLUSION

This paper discussed the characteristics of the LC Delay Line oscillator: frequency of operation, mismatched termination, phase shift, and the voltage amplitudes. The theoretical calculations that were made were pretty close to the experimental values. (less than 10% error) Later in the paper, other oscillator alternatives were tested and briefly discussed: The ECL oscillator improved the operating frequency while the Tunnel Diode oscillator did not function.

Later on in this paper, the LC Delay Line oscillator was compared to the SAW oscillator. There is no reason to beleive that these two oscillators are comparable. The SAW oscillator's operating frequency is much higher than the other and its stability is superior. This is like comparing a Volkswagon to a Porche.

An attempt was made to make the actual device oscillate, but this failed. Due to time limitations, this could not be investigated further.

The scope of this paper on this subject is somewhat limited, but I hope that the reader has gained an understanding of the basic principles of delay lines used as oscillators.

9.0 BIBLIOGRAPHY

"General Characteristics of Delay Lines." Bel Fuse Inc.

"Delay Line Catalog." PCA Electronics Inc.

Bell,D. "Surface-Acoustic-Wave Resonators" IEEE Journal, Vol. 64, No. 5, (1976), 711-720

Dobson,R. " An introduction to the design of Surface Acoustic Wave devices." Defence Research Center Salisbury South Austrailia Technical Report AEL-0001-TR

EVALUATION OF A SURFACE ACOUSTIC WAVE RESONATOR MANUFACTURED AT SAN JOSE STATE UNIVERSITY

by

Dipl. Eng. Andreas Gulle

Supervisor: Prof. Udo Strasilla

Department of Electrical Engineering
San Jose State University

15 Dec. 1983

NASA Grant NAG 2-85

EVALUATION OF A SURFACE ACOUSTIC WAVE RESONATOR MANUFACTURED AT SAN JOSE STATE UNIVERSITY

by

Dipl. Eng. Andreas Gulle

Supervisor: Prof. Udo Strasilla

Abstract

Three Surface Acoustic Wave Resonators with different geometries manufactured in the SJSU Integrated Circuits Laboratory were evaluated. In order to better analyze their features they were compared with commercial SAW devices. In the first device no useful measurements could be achieved due to the fact that the distance between the interdigital transducers (IDT's) was too large and because only two electrode pairs could not couple a sufficient signal. The second SAW with an increased number of electrode pairs (15) and the same number of reflectors showed a frequency characteristic with a center frequency near the required 180 MHz frequency indicating proper spacing. However the Q value was rather poor vending the device useless in an oscillator configuration. In the third device, where the reflectors were omitted, the importance of reflectors were demonstrated. The frequency characteristic of this device was poor due to the superposition of uncontrolled randomly reflected waves from the edge of the device.

The study shows that the signal strength and Q-value will be increased greatly if the IDT's are spaced close for sufficient coupling and if a high number of reflectors, preferably grooved, are used in order to create a standing wave. Due to limited equipment for the UHF-range no observations of the sine wave was possible.

That a SAW device can be used for stabilizing the oscillation frequency of a resonating circuit was demonstrated by using a commercial high Q 280 MHz resonator from Hewlett Packard in a common-base Colpitts configuration. The advantage of using a SAW device for oscillator stabiliaztion is obvious when considering that the 11th harmonic of a bulk acoustic wave crystal would have to be used in order to achieve the same oscillation frequency.

EVALUATION OF A SURFACE ACOUSTIC WAVE RESONATOR MANUFACTURED AT SAN JOSE STATE UNIVERSITY

by

Dipl. Eng. Andreas Gulle

Supervisor: Prof. Udo Strasilla

Table of Contents

I. Introduction

Usually oscillators use crystals operating in the bulk mode in order to stabilize the frequency. The problem is that bulk-acoustic-wave resonators (BAWRs) can only work up to the range of 50 MHz[1]. If one needs higher frequencies the harmonics can be used, or a frequency multiplication network may be added. A multiplication network often takes too much space in a certain design. The use of the crystal's overtones are limited by the low amplitude (high loss in the BAWR). Basically due to the low amplitude the oscillator circuit cannot be stabilized enough (eg. using the 10th overtone).

Those problems can be overcome by using a SAWR. Its frequency abilities range from 50 MHz to 1 GHz[2].

[1] hp-journal p. 14.

[2] hp-journal p. 14.

II. Theory of the SAWR

The key elements are the interdigital transducer (IDT). It couples the electric signal to the crystal and produces the acoustic wave. The acoustic wave travels on the surface of the crystal (bulk waves are also produced) to a second IDT. This transforms the acoustic wave back to an electrical signal.

This mechanism becomes useful for a frequency selective device. There will be only a fairly small frequency range where a good coupling occurs. This resonant frequency depends on the spacing of the fingers of the transducer.

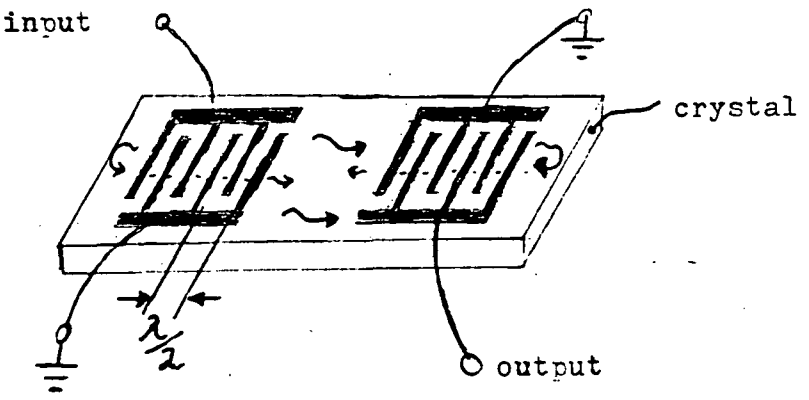

Figure 1: Principle of a SAWR

The IDT sends waves to all directions. They will be reflected at the edges of the crystal. These reflected waves (see Fig. 1) will interfere in a random way with the main wave. In order to eliminate that problem an array of reflectors is used.

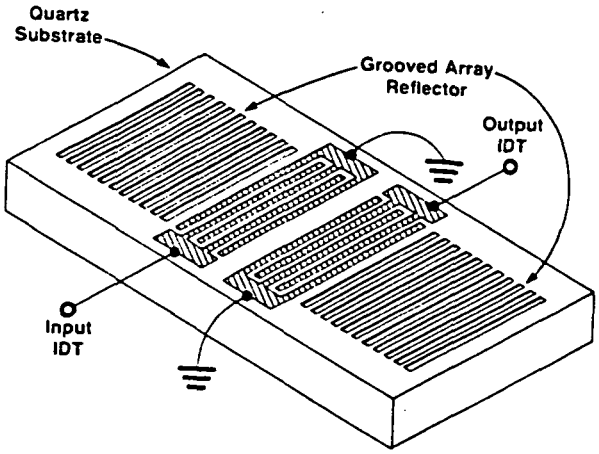

Two-port surface-acoustic-wave resonator. The arrays of grooves at each end reflect the surface waves excited by the input IDT. The reflected waves constructively add at a frequency largely determined by the periodicity of the grooves.

Figure 2: Two-port SAWR[1]

"The arrays of grooves at each end reflect the surface waves exited by the input IDT. The reflected waves constructively add at a frequency largely determined by the periodicity of the grooves"[1]. If there are enough reflectors at both ends with an appropriate spacing ($\lambda/2$) there will be created a standing wave. This standing wave will give a very sharp resonance peak (very high Q) with a steep slope of the phase. This will lock in the frequency of an oscillator and stabilize it very accurately to the resonance frequency of the SAWR.

[1] hp-journal p. 9.

III. The Equivalent Circuit

The equivalent circuit of the SAWR is a series resonance circuit (with effective components L_1, C_1, R_1) parallel with a capacitance (C_0) due to the IDT.

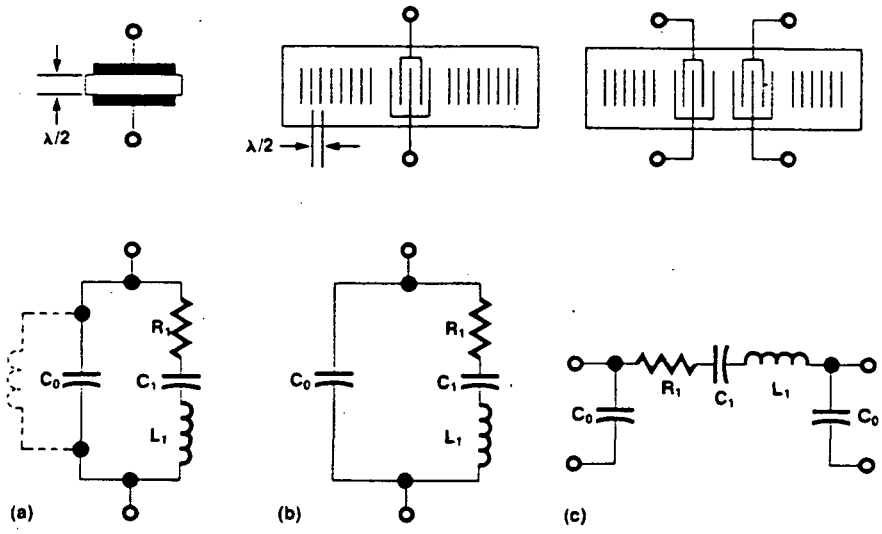

Figure 3: Crystal resonator geometries and equivalent circuits.
(a) One-port, bulk-acoustic-wave resonator.
(b) One-port surface-acoustic-wave resonator.
(c) Two-port surface-acoustic-wave resonator.

For a one-port device (b) the capacitance C_0 has to be compensated with an external inductor (L_{ex}) resonating at the resonance frequency.

$$f_0 = \frac{1}{2\pi\sqrt{L_1 C_1}} = \frac{1}{2\pi\sqrt{L_{ex} C_0}}$$

In addition, parasitic capacitance exists between the leads and the package.

[1] hp-journal p. 10

IV. Evaluation of Commercial Devices for Comparison

For comparison two commercial devices were studied. One was the CTI91 44 MHz intermediate frequency filter from Crystal Technology. The other was the hp 1GA1 280 MHz SAWR.

a. The hp 280 MHz SAWR

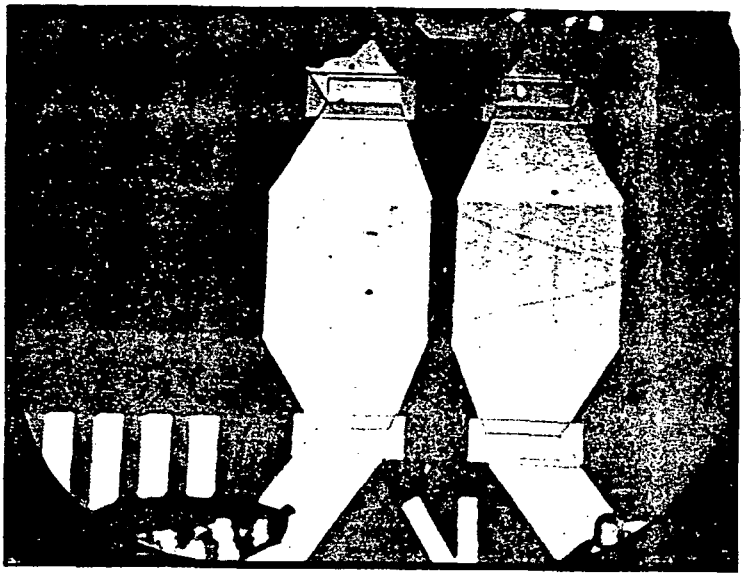

a) Total view

b) Closeup view

Figure 4: Picture of the hp 280 MHz SAWR

The array of grooves working as reflectors is seen as a grey band.

The hp 280 MHz SAWR is bonded as a one port device. Therefore the capacitance C_o due to the IDT's is a dominating factor (see equivalent circuit). This capacitance determines the response outside the resonant frequency.

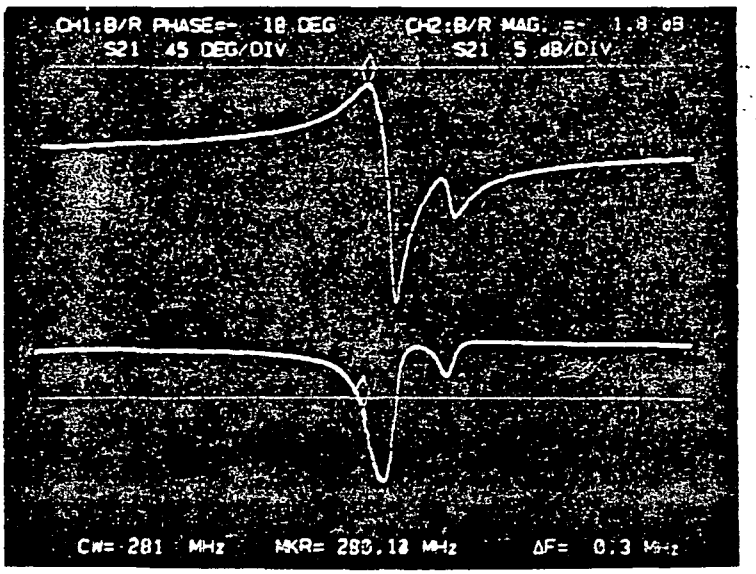

reference: -2dB

5dB/Div

f_0 = 280.14 MHz

50 kHz/Div

Figure 5: Picture of the frequency and phase response of the hp 280 MHz SAWR.

The first positive peak occurs at the resonancepoint of the series resonance circuit which is the desired frequency of 280 MHz. (This device is 140 kHz off and was therefore rejected by the Hewlett Packard Quality Control Dept.) In that case C_0 is almost shorted out since only the low R_1 limits the feedthrough.

The negative peak occurs when C_0 and L_1 resonate as a parallel resonance circuit giving a low feedthrough ($\rightarrow$0).

The second positive hump indicates a side mode. This can be modelled by a second series resonance circuit with a much higher R_2.

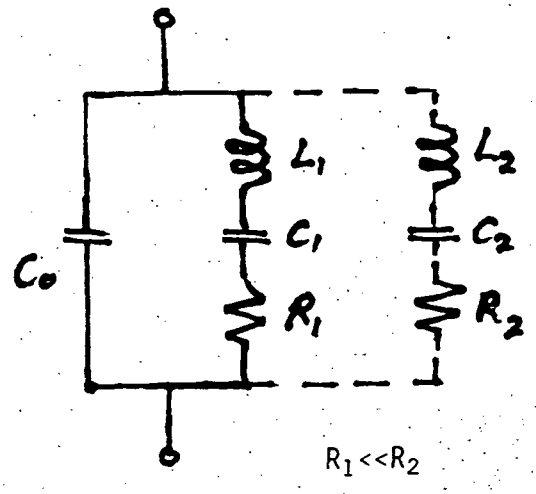

Figure 6: Equivalent circuit for the hp 280 MHz SAWR

The insertion loss of about -2dB shown in the picture agrees with the data specifications.

It is obvious that the peaking at the resonance frequency is not high enough above the level outside the resonance frequency. This level is due to C_o. As it is later shown in the oscillator design, the C_o has to be compensated by an external inductor.

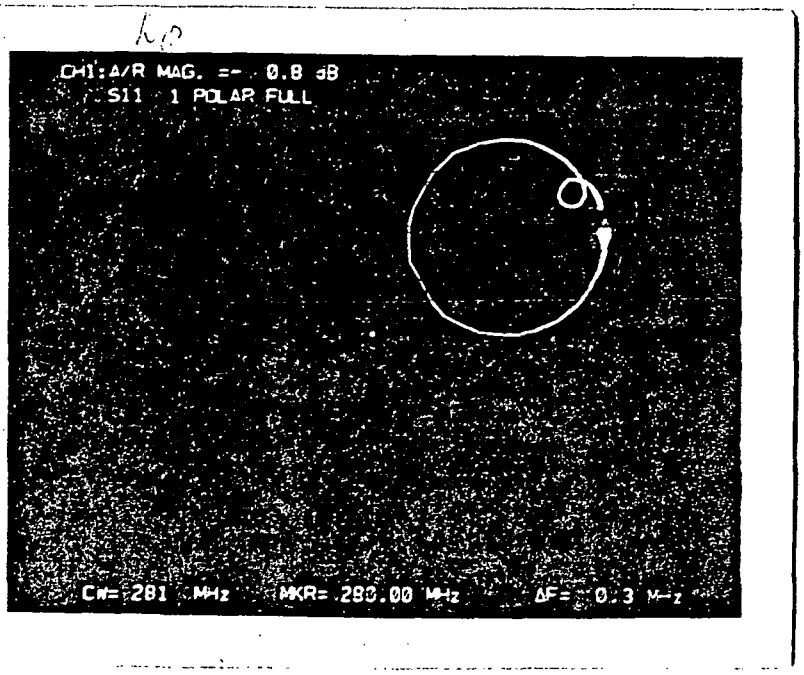

Figure 7: Picture of the input impedance (transfer locus) of the hp 280 MHz SAWR.

Since the hp 280 MHz SAWR is connected as a one port device one gets a different input impedance character than looking into a two port (see equivalent circuits). While the input of a two port is dominated by C_0 the hp device shows an inductive characteristic.

By the very thin trace of the main loop (main resonance) a fast phase shift is indicated. This agrees with the phase plot in Figure 5. There is also an agreement between Figure 5 and Figure 7 by the indication of the secondary resonance point as shown in the small loop.

The impedance around the main resonance point becomes real. The highest value given in data specifications[1] is 60 Ω (typically 35 Ω). This is normalized for 50 Ω: 60 Ω/50 Ω = 1.2. The picture shows 2.4 · 50 Ω = 120 Ω to 4.0 · 50 Ω = 200 Ω as real impedance. This difference in the real part is most probably due to real losses in the fixture. Omitting that error, the curve in the S_{11}-plane lies closest to the center point (1 in the impedance plane responding to a reflection coefficient of $\Gamma=0$).

b. The CTI 91 Filter

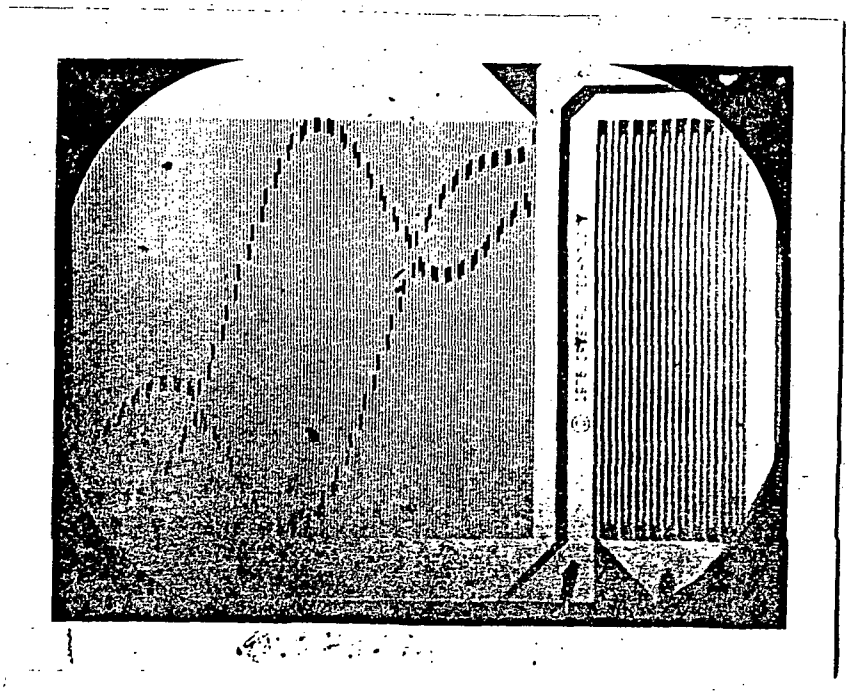

Figure 8: The IDT's of a CTI 91 intermediate filter

[1]hp-journal p.15

It can be clearly seen that the input IDT on the left hand side is different from the output IDT on the right hand side. The different length of the electrodes of the input IDT shapes the filter characteristic.

The CTI 91 is bonded as a two port device. Here the IDT capacitances C_o are seen at each port. (See equivalent circuit). This has to be considered by looking at the impedance of the ports.

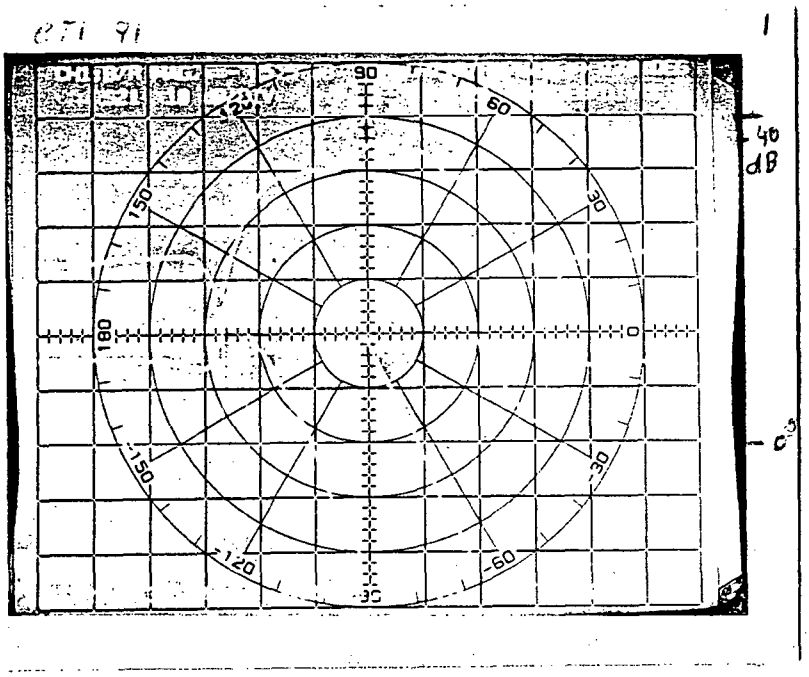

a) measured

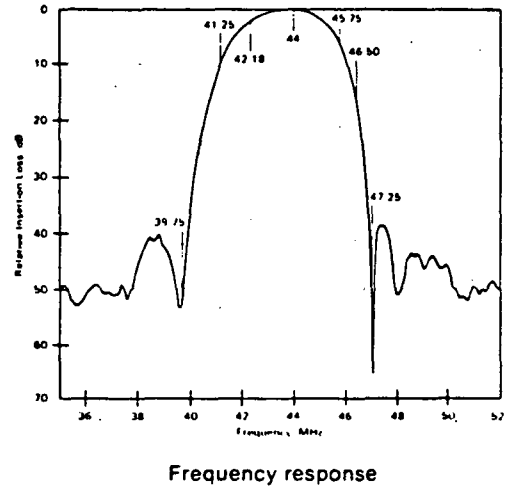

b) data specifications[2]

Figure 9: Frequency and phase response of the CTI 91 Filter

The device is designed as an IF-Filter rather than a resonator. Therefore its response shows a broader bandwith than the hp device. The tested device shows a bandwidth of ca. 5.5 MHz while the bandwidth given in the data specifications is 6.6 MHz.

[2]Crystal Technology data specification

The high insertion loss is a result of a failure in the fixture as later discovered.

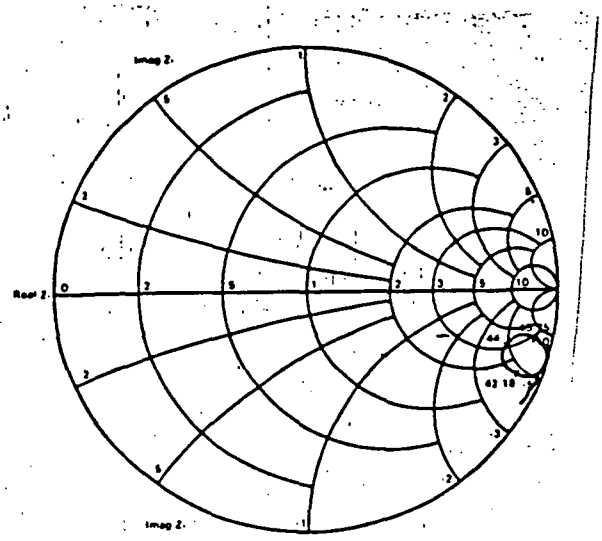

Input impedance (normalized to 50Ω) Zi
vs frequency (Zi = 0)

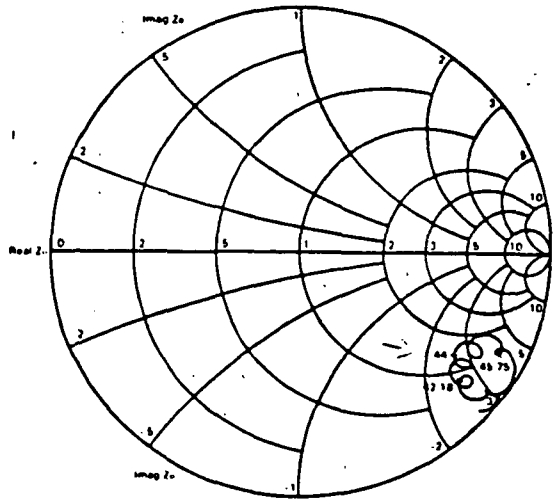

Output impedance (normalized to 50Ω)
Zo vs frequency
(input conjugate matched)

Figure 10: Input (a) and output (b) impedance given in the data specification[2].

Due to the design of the CTI 91 (see Fig. 8) the S_{11} and S_{22} plane look different. Beside the resonance frequency, both the input and output show an almost lossless capacitive character. It is obvious that the device has to be operated with a conjugate matching circuit in order to convey the transfer locus close to the reflection less point $\Gamma=0$ in the center of the Smith chart.

[2] Crystal Technology data specification

V. The Devices Manufactured at SJSU

The requirement is to manufacture a SAWR with a resonance frequency of 180 MHz. This target has to be met in steps.

So far three designs have been made. Two with a 10 μm spacing in the Integrated Circuit laboratory of SJSU and one with 5 μm technology using outside facilities to produce the mask. All designs use $LiNbO_3$ as crystal material. With a velocity of 3600 m/s the expected frequency can be calculated as follows:

$$f_o = \frac{V}{2d}$$

where d is the distance of an electrode pair.

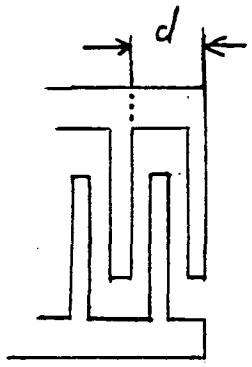

This gives for

10 μm spacing d=40 μm, therefore

$$f_o = \frac{3600\ m/s}{2 \cdot 40\ \mu m} = 80\ MHz$$

and for

5 μm spacing d=20 μm, therefore

$$f_o = \frac{3600\ m/s}{2 \cdot 20\ \mu m} = 180\ MHz$$

The following analysis was done with an HP-network analyzer.

a) First run, SAW1

For the first run two electrode pairs and seven reflectors were

used. The distance between the IDT's was 780 μm.

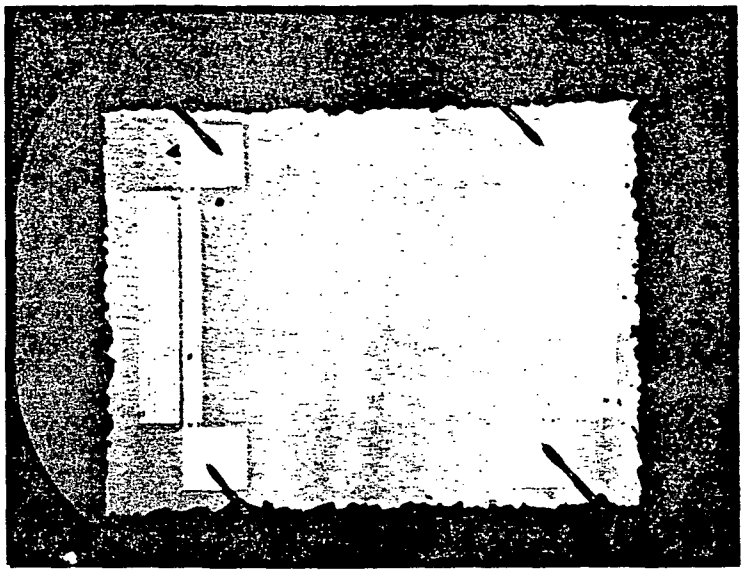

Figure 11: Picture of the first device (called SAW1)

No useful measurements could be achieved with this device since the long distance between the IDT's has a too high loss. Also two electrode pairs are not efficient enough to couple a sufficient signal.

b) Second run, SAW2

In the second step the electrode pairs were increased to 15 (N=15). The number of reflector strips remained at seven. The space between the IDT's was reduced to 420 μm.

The distance of the electrode pairs points towards an expected bandwidth of approximately:

$$\frac{\Delta f}{f_0} \approx \frac{1}{N}$$

$$\Delta f \approx \frac{f_0}{N} = \frac{80\ \text{MHz}}{15} = 5.3\ \text{MHz}$$

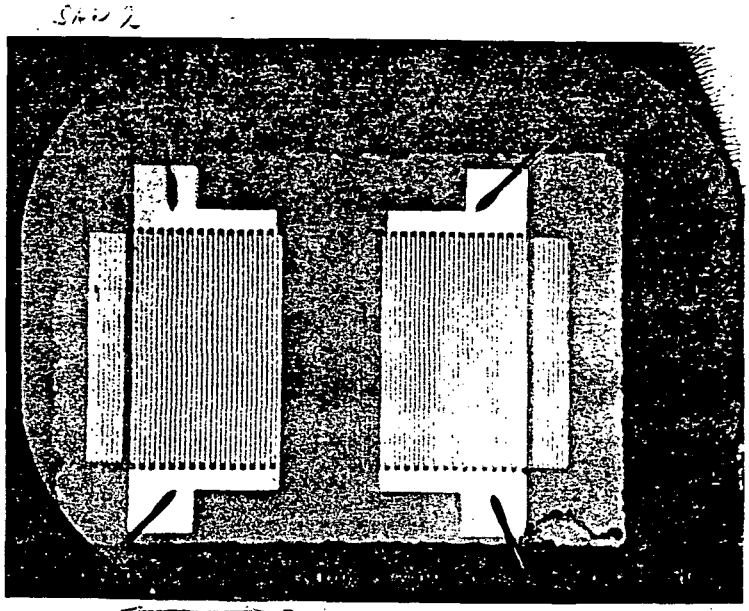

Figure 12: Picture of second device (SAW2)

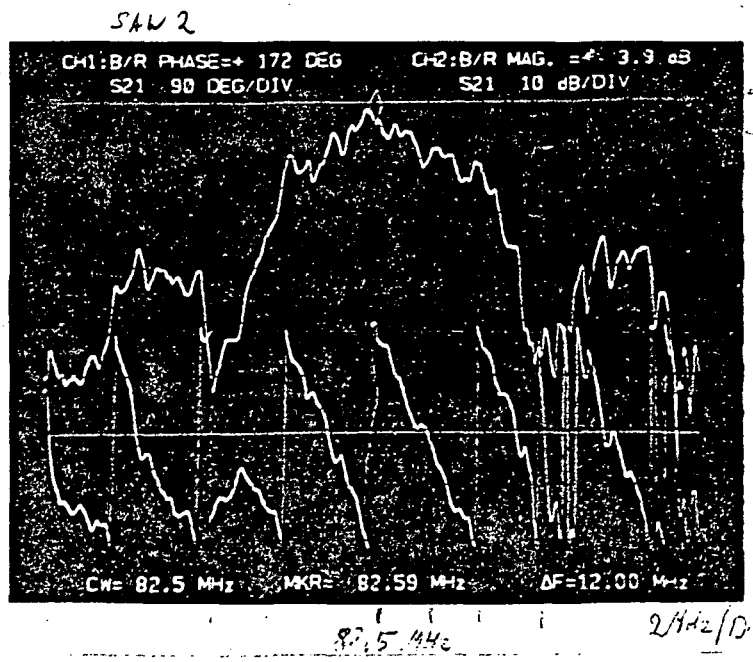

reference:

-10dB

10db/Div

f_o = 82.5 MHz

2 MHz/Div

Figure 13: Frequency and phase response of a SAW2

The transfer function shows the center frequency is about 3 MHz higher than that designed for. The bandwidth with about 8 MHz is about 3 MHz wider than estimated.

For a SAWR the bandwidth is much too wide and the phase not steep enough.

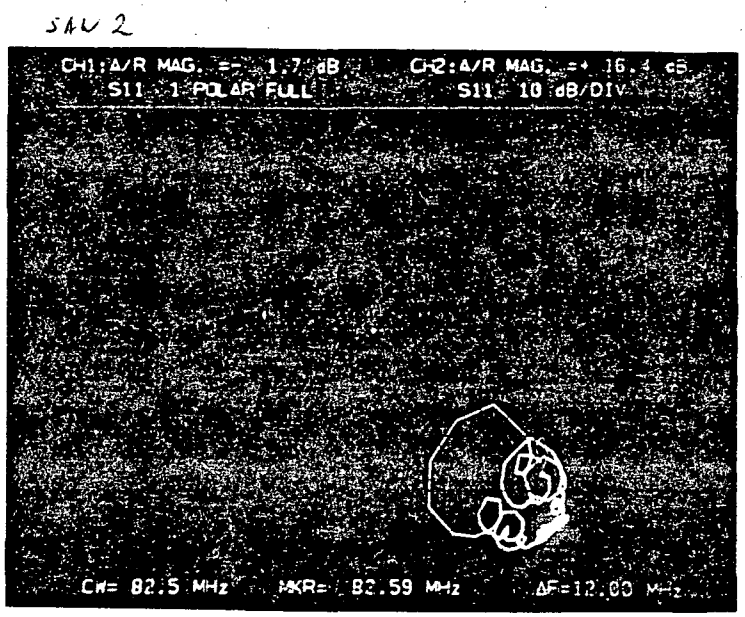

Figure 14: Input impedance of a SAW2

It can be seen that, near the main resonance (large loop) many secondary resonance points (secondary loops) occur. This agrees with the S_{21} picture which shows many small peaks. This is most likely due to a travelling wave with random superposition.

As predicted by the equivalent circuit the device bonded as two port shows a strong capacitive characteristic (due to C_0).

c) Third run, SAW3

The third design was meant to meet the required 180 MHz resonance frequency. As seen, this requires a spacing of 5 μm for the IDT electrodes, exceeding the capability of the masking facilities at SJSU

to produce masks with this spacing. Therefore the masks were produced in facilities of a Silicon Valley company.

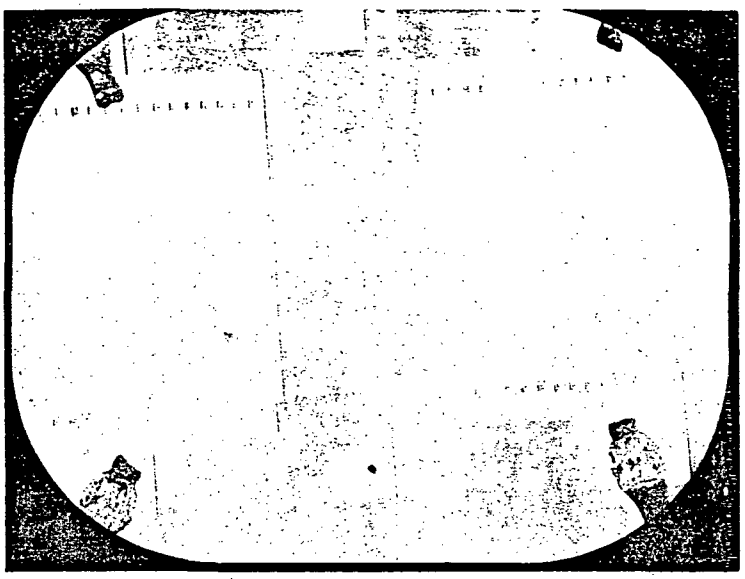

Figure 15: Picture of the third device (SAW3)

This time, reflectors were omitted in order to study the pure effect of the IDT's. Again 15 electrode pairs were used. Therefore the expected bandwidth is

$$\Delta f = \frac{180\ \text{MHz}}{15} = 12\ \text{MHz}$$

The distance between the IDT's is 210 μm.

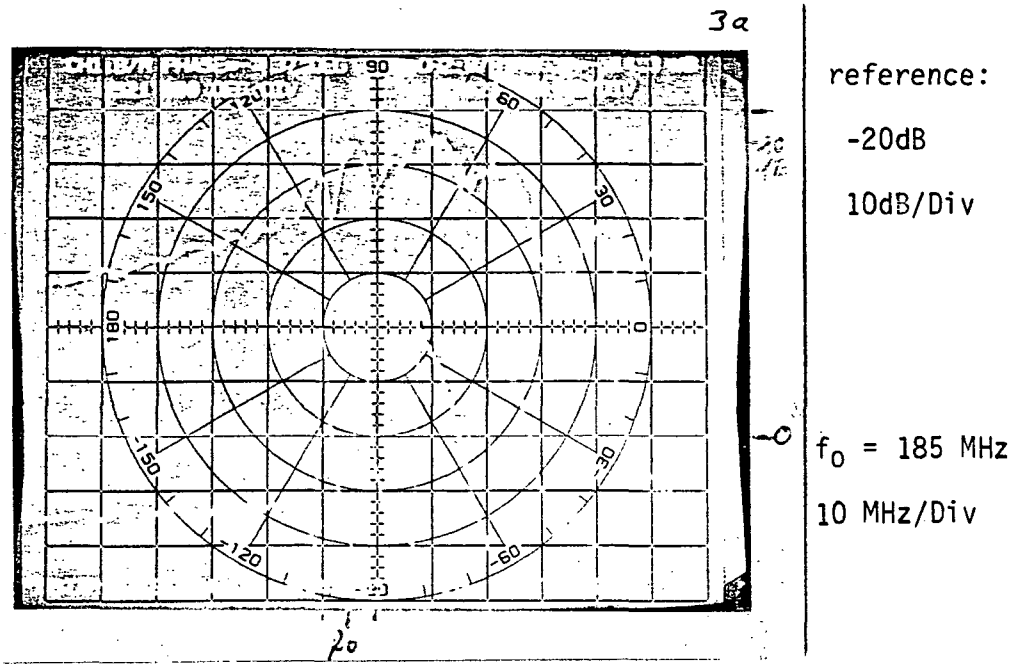

Figure 16: Frequency and phase response of a SAW3

As expected the frequency response does not show a distinct resonance peak. The main peak occurs with about 185 MHz, 5 MHz above the designed frequency. Its bandwidth, about 10 MHz, is relative close to the expected 12 MHz. Here the full range of such effects are obvious, which have to be eliminated in order to get a usable resonator.

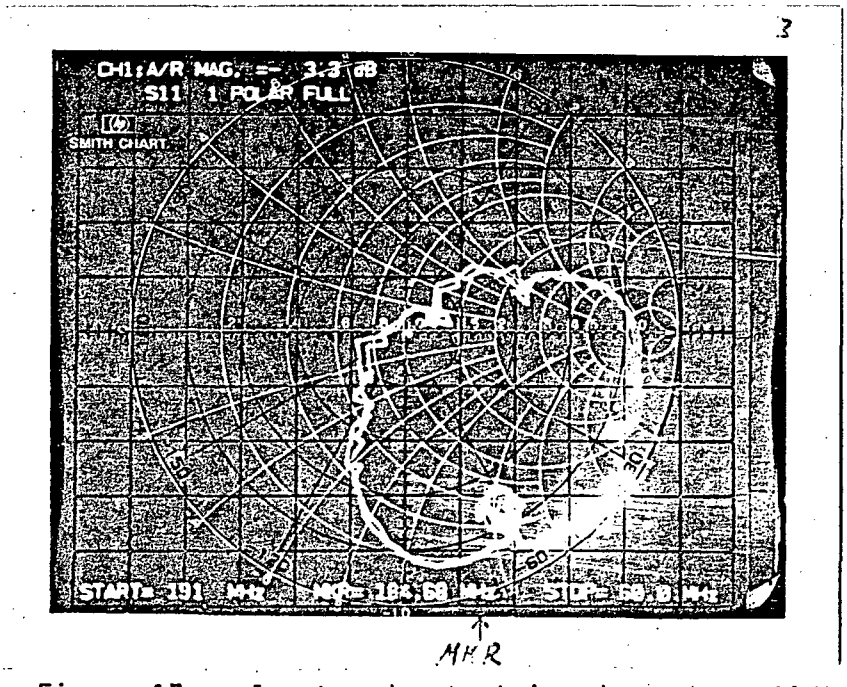

Figure 17: Input and output impedance of a SAW3

As expected from viewing the frequency response the transfer locus is full of wiggles and side loops. At the resonance frequency occurs the largest loop.

Here S_{11} and S_{22} are shown on top of each other indicating the symmetry of the device. The impedance of both parts start off with the character of an almost lossless capacitance. At frequencies higher than the resonance peaks it becomes inductive. When the phase shift becomes zero again the impedance shows a capacitive character again. There are two frequencies where a real impedance occurs. The first is very close to the point of complete matching [point 1 in the impedance plane (center point) indicates a reflection factor of $\Gamma=0$].

In order to see the effect of reflection at the edges of the crystal, wax was applied at the crystal edges. The wax absorbs the surface acoustic waves.

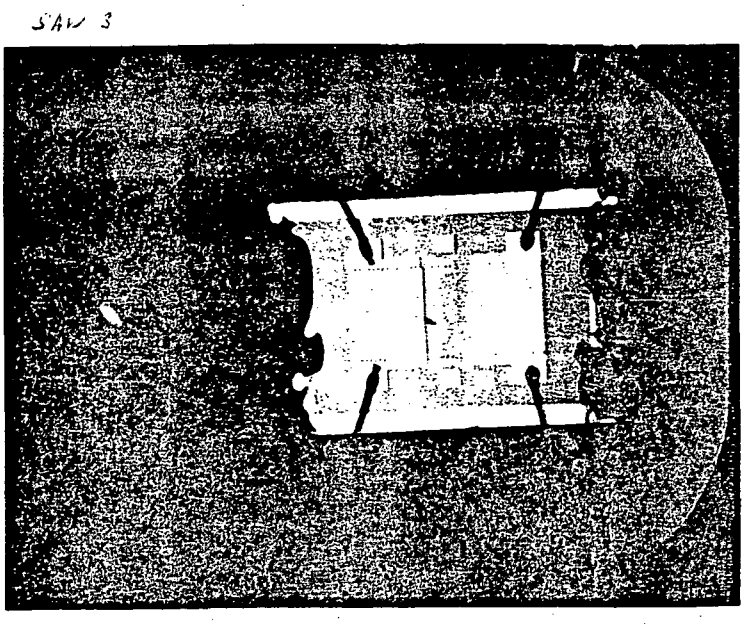

Figure 18: Picture of a SAW3 with wax applied

The result can be seen in the following picture:

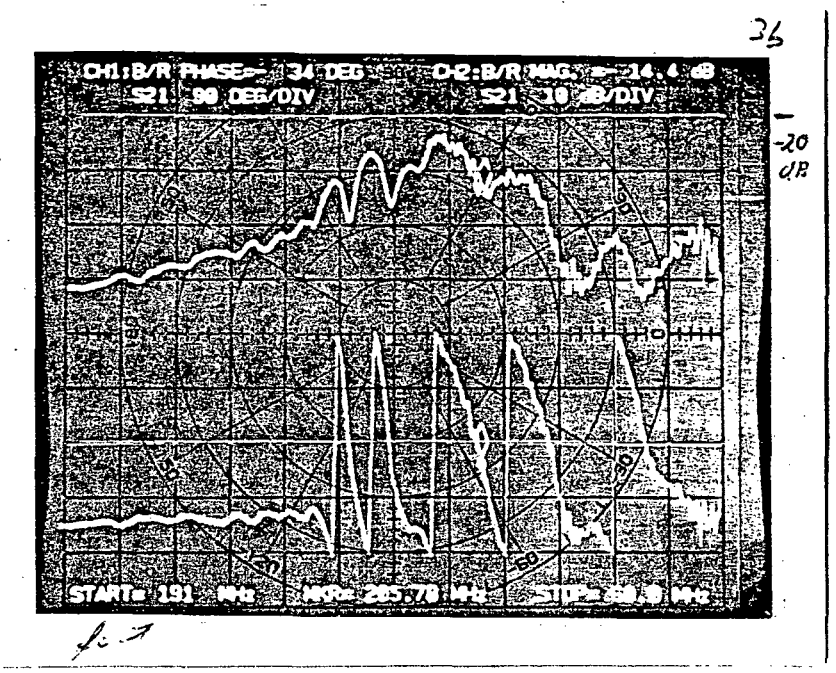

Figure 19: Frequency and phase response of a SAW3 after the wax was applied.

Mostly the ripples in the main peak were prevented by the application of the wax.

IV. Discussion

The results show that the frequency range of the device is determined by the spacing of the IDT's. In order to reduce the loss the IDT's have to be close enough for sufficient coupling.

The most important step is the design of the reflectors. By omitting the reflectors, travelling waves are created which are randomly reflected at the edges of the crystal. Due to a random superposition the waves are subtracted and added randomly. By introducing some reflectors those effects decrease and a resonance peak occurs. In order to create a narrow band resonance peak a fairly high number of reflectors is needed as seen in the commercial devices. If the number of reflectors is high enough a standing wave will be created. This will give a high Q device.

In order to meet the requirements for a 180 MHz resonator the necessary step is to design a device with enough reflectors so that a standing wave will be created. As learned from discussions with experts from industry a good approach will be about 100 reflectors. As shown, the spacing of 5 μm gives the wanted frequency range by using $LiNbO_3$ as substrate.

VII. Appendix

A 280 MHz oscillator stabilized with a SAWR

In order to gain the knowledge how to use a SAWR for stabilizing an oscillator circuit an hp 280 MHz SAWR was used.

In general there are two commonly used circuit configurations. One (a) is for a SAWR packaged as a two port and one (b) for a SAWR packaged as a one port.

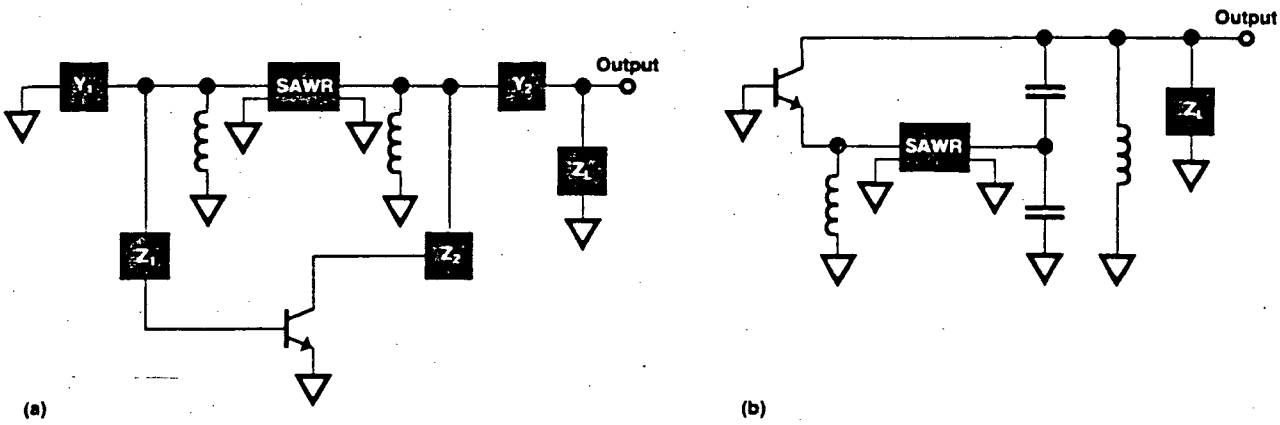

SAW oscillators using two-port SAWRs in a common-emitter or Pierce circuit (a) and a common-base circuit (b).

Figure 20: SAW oscillator circuit configurations[1]

The common-emitter (or Pierce) type (a) achieves in general better results but requires relatively exact inductors "to remove the reactance (at resonance) caused by IDT capacitance.[1]" Further, an impedance matching network is needed.

The common-base configuration "is only conditionally stable which leads to ... a higher noise floor far away from the fundamental signal[1]" but has less noise near the resonant frequency than the common-emitter type.

[1] hp-journal p.17, p.16.

Due to the accessibility of a one port device, the common base configuration was chosen. An application was found in the 280 MHz intermediate frequency oscillator of the HP 8558 spectrum analyzer. There is an eleventh overtone BAWR substituted by a SAWR for better stability.

Analysis

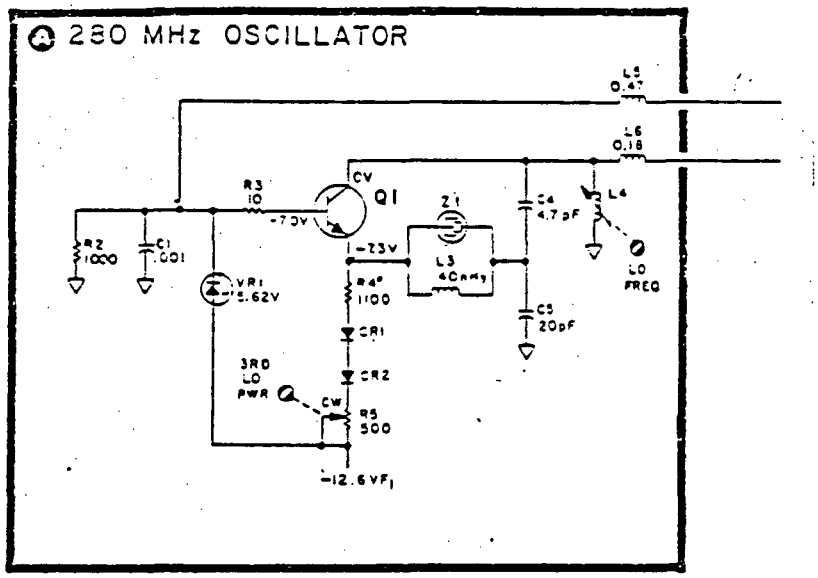

Figure 21: Modified IF 280 MHz oscillator of a HP 8558 spectrum analyzer

The circuit is based on a Colpitts configuration. The SAWR is in series to the input of the amplifier.

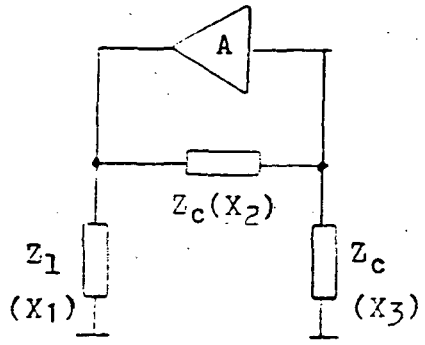

a) Shematic of a Colpitts-oscillator

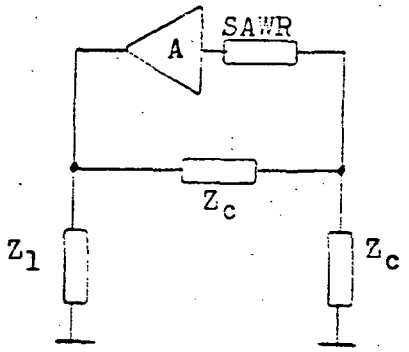

b) Colpitts-oscillator with a SAWR

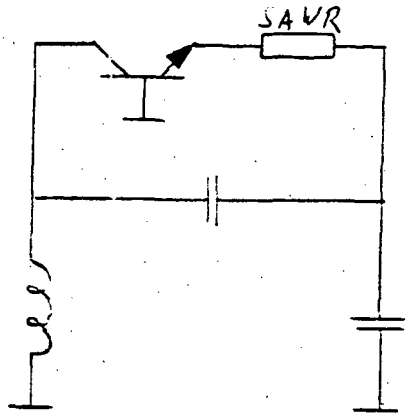

c) AC- configuration of the circuit

Figure 22: Development of the circuit analysis

The conditions for oscillations are:

Gain: $$A_{cr} = -\frac{X_1}{X_3} = \frac{X_2 + X_3}{X_3}\ ;\ \text{and}$$

Phase: $$X_1 + X_2 + X_3 = 0.$$

Therefore:

$$A_{cr} = -\frac{\omega_o L}{-1/\omega_o C_5} = \frac{\omega_o C_4 + \omega_o C_5}{\omega_o C_5}$$

$$A_{cr} = \frac{C_4 + C_5}{C_5}$$

and

$$-\frac{1}{\omega_o C_4} - \frac{1}{\omega_o C_5} + \omega_o L = 0$$

$$\omega_o L = \frac{1}{\omega_o}\left(\frac{1}{C_4} + \frac{1}{C_5}\right) = \frac{1}{\omega_o C_5} \; ; \text{ where } \frac{1}{C_5} = \frac{1}{C_4} + \frac{1}{C_5}$$

$$L = \frac{1}{\omega_o^2 C_5}$$

Using the values of the circuit:

$C_5 = 20pF \,||\, 5pF = \underline{4.0pF}$

for 280 MHz:

$$L = \frac{1}{\omega_o^2 \cdot 4.0pF} = \underline{\underline{80.7\ nH}}$$

$$X_L = \omega_o L = \omega_o \cdot 80.7\ nH = \underline{142\Omega}$$

This gives a sufficient gain for the base configuration

$$A_{cr} = \frac{20pF + 5pF}{5pF} = 5$$

Due to parasitic capacitance the inductor L = 80 nH → 90 nH (2½ turns of copper ϕ 40 mil ≈1mm around an RF-core) had to be reduced to 1½ turns. The value of this inductor could not be measured any more.

By trial and error an appropriate inductor was found to couple the output to a 50Ω load. The circuit performance became excellently stable.

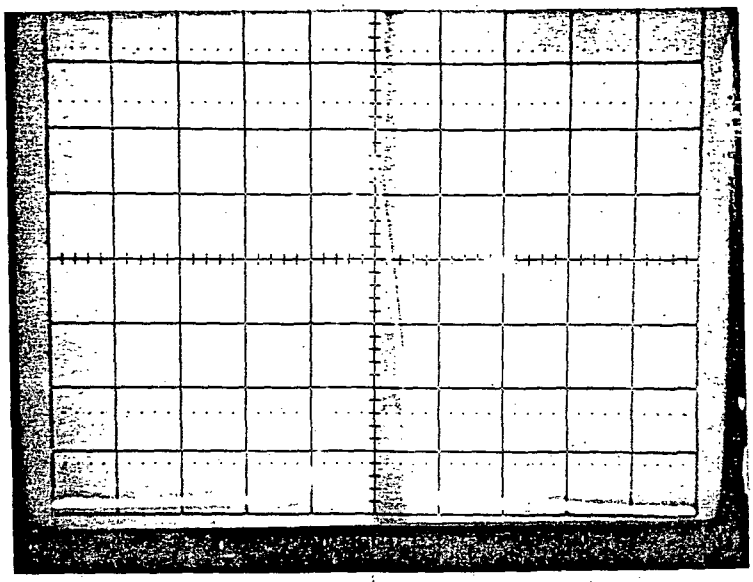

Figure 23: Picture of the oscillating frequency observed with an HP 8557A spectrum analyzer

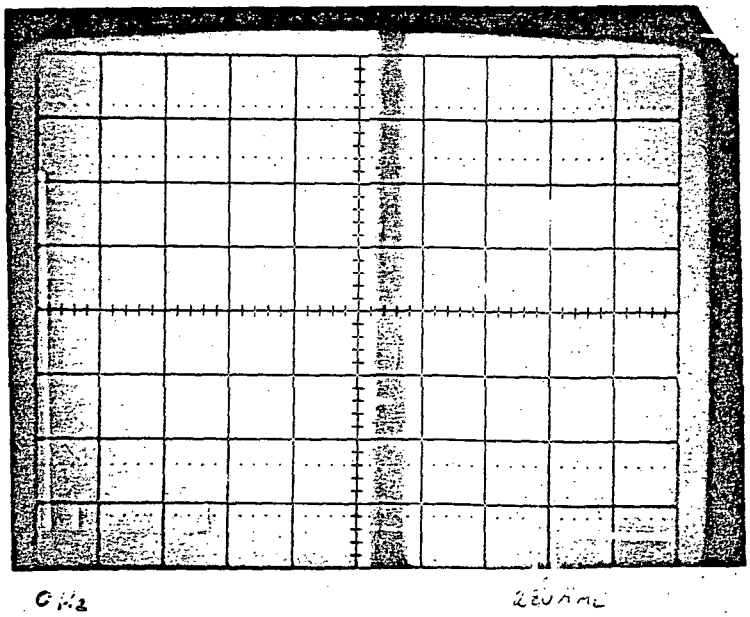

Figure 24: Picture of the entire spectrum

References

A. Hewlett Packard Journal, December 1981.

B. Data Sheets on CTI 91 and CTI 558 SAW Filters, Crystal Technology Inc., 1035 East Meadow Circle, Palo Alto, California 94303.

Acknowledgement

We thank Mr. William R. Shreve at Hewlett Packard for his support and help which made this evaluation possible.

Funding for this project was provided by NASA grant NAG 2-85 whose support is gratefully acknowledged. The experimental SAW devices were manufactured by Prof. Chen Yuen, Department of Electrical Engineering, San Jose State University, under NASA grant NCC 2-143.

Application of Surface Acoustic Wave Devices to Radio Telemetry

Interim Status Report
covering period
1 Feb. 81 to 30. Sept. 81

Principal Investigator: Udo Strasilla
Assoc. Professor
Dept. of Electrical Engineering
San Jose State University
San Jose, Calif. 95192

Grant No. NAG 2 - 85

Report submitted to: Gordon J. Deboo
Chief, Electronic Instrument
Development Branch
Mail Stp 213-3
Ames Research Center
Moffett Field, Calif. 94035

Application of Surface Acoustic Wave Devices to Radio Telemetry

(Interim Status Report covering period 1. Feb. 81 to 30. Sept. 81)

The purpose of the project is:

1. the procurement of a commercially available SAW resonator,
2. the reconstruction and experimentation with conventional oscillators to gain more experience with different oscillator configurations and with the operations of these in the 100 MHz region,
3. the construction and evaluation of an oscillator using a SAW resonator.

The results up to now in regard to the proposed phases are summarized below:

Phase 1 - Procurement of resonators

Up to now we were unsuccessful in obtaining commercial SAW resonators. The following firms involved in the manufacture of SAW devices were contacted: Anderson Labs. Inc., Crystal Technology, Kyocera International, Plessey Semiconductors, Rockwell International, SAWtek Inc., Hewlett Packard, and Crystek Corporation. Though many of above companies make SAW devices, they concentrate on the high volume market of filters, TV delay lines etc. Only some companies made resonators (Crystal Technology and HP, for example), however, only for internal research. Many companies are now trying to assess the potential market for SAW resonators, and will come up with products only if there exists a high volume potential.

A visit of the manufacturing and testing facility of Crystal Technology at Palo Alto convinced us that this company is strongly committing itself to SAW devices in general. Funded by their new parent company Siemens, they purchased new fabrication equipment expanding to new facilities this fall.

From Crystal Technology SAW bandpass filters were obtained: the CIT 55B and the CTI 91 with center frequencies of about 65 MHz and 45 MHz, respectively. Experimentation with these devices are in progress to gain familiarity with the measurement problems of SAW devices in the greater than 40 MHz region (see second part of status report by Michael Williamson).

Phase 2 - Experimentation with different oscillators

Two students are involved in this phase: Michael Williamson and Timothy Upshaw. Their results are described in their informal interim status reports attached.

Williamson experimented with a conventional crystal controlled oscillator similar as that used by Ames Research in some of their radio telemetry applications. He used the third harmonic of the 20 MHz crystal controlled oscillator to achieve 60 MHz oscillation. Measurements on the Crystal Technology SAW filter CTI 55B with the interdigit pattern shown in Fig. 1 are now underway.

Upshaw simulated a SAW delay line by using a tapped lumped element LC delay line, where the tapped output was fed back to the input via a NAND gate, producing oscillation where the frequency depended on the effective length of the delay line (or on the tap used). It appears that this scheme of making an oscillator with different fixed frequencies can be also realized with a SAW device, provided that a device is fabricated with multiple output ports, each at a different distance from the input port.

In addition, other oscillators were designed and constructed, for example the Wien Bridge oscillator and phase shift oscillator. Though these circuits operate in the audio range, they served the purpose of studying the fundamentals of oscillator design, and they could be used for demonstration in a senior circuit design course at San Jose State University (EE 124).

Phase 3 - Construction and evaluation of oscillator using SAW resonator

This phase was not started yet, partially due to the nonavailability of commercial SAW resonators. Due to the fact that there is no hope in obtaining resonators this year, it is fortunate that another research grant was awarded to Prof. Chen Yuen at SJSU, which is concerned with the fabrication of SAW resonators.

In an initial attempt Prof. Yuen fabricated a SAW resonator with the pattern shown in Fig. 2. This is being packaged at Crystal Technology. When this device will be available we can proceed with the third phase of the project, as outlined in the project proposal. Though this initial device is only a first order approximation of the desired resonator, it will serve well the purpose for developing measurement techniques: for example delay measurements, insertion loss and distortion measurements. Finally the different oscillation schemes will be tried, like the one with the amplifier in the feedback path and the other with the NAND gate, and the performance will be evaluated.

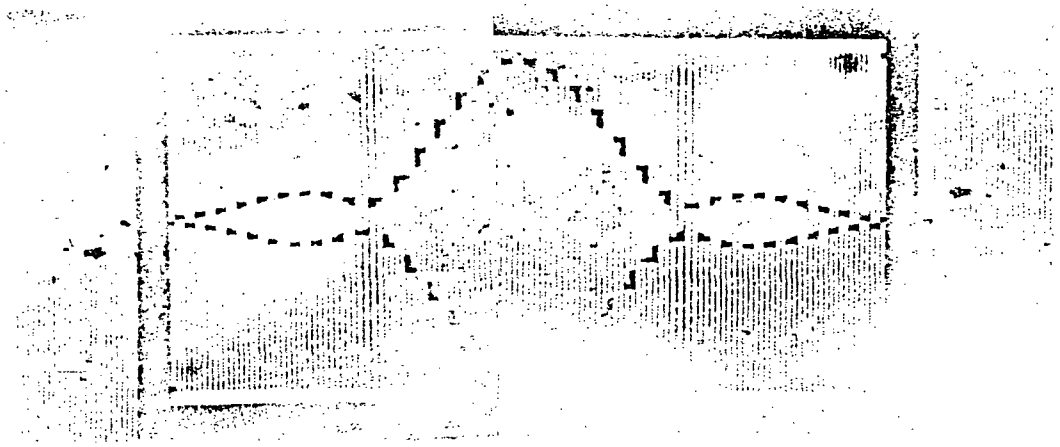

Fig. 1 Interdigit Pattern of Crystal Technology
CTI 55 B SAW Bandpass Filter (65MHz)

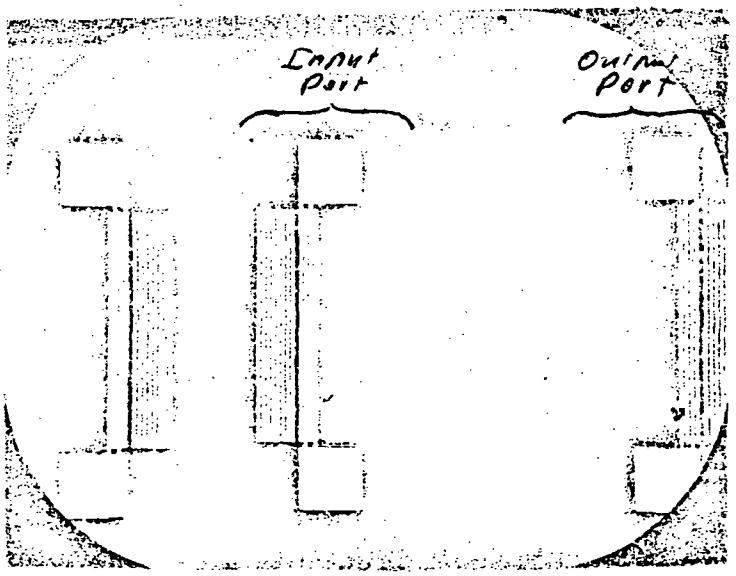

Fig. 2 Interdigit Pattern of Potential SAW
Resonator Fabricated by Prof. Yuen (SJSU)